

# Infragravity waves in Dutch tidal basins and estuaries

Implications for flood risk assessment



# **Infragravity waves in Dutch tidal basins and estuaries**

## Implications for flood risk assessment

### **Author(s)**

Jacco Groeneweg (DELTA RES)

Ad Reniers (TU Delft Faculteit Civiele Techniek en Geowetenschappen)

Joana van Nieuwkoop (DELTA RES)

## Infragravity waves in Dutch tidal basins and estuaries

Implications for flood risk assessment

<b>Client</b>	Rijkswaterstaat Water, Verkeer en Leefomgeving
<b>Contact</b>	Marieke Hazelhoff
<b>Reference</b>	SITO-PS 2025 WVH08 – KvK HB7-2: effect IG golven op mechanismen dijkerosie Plan of Approach "Golfoploop en -overslag ondiepe voorlanden" – revision, d.d. 16 July 2025
<b>Keywords</b>	Infragravity waves, estuaries, SWAN, wave run up, wave overtopping, flood risk

### Document control

<b>Version</b>	1.0
<b>Date</b>	03-02-2026
<b>Project nr.</b>	11211572-021
<b>Document ID</b>	11211572-021-GEO-0001
<b>Pages</b>	38
<b>Classification</b>	
<b>Status</b>	Final

### Author(s)

	Jacco Groeneweg Ad Reniers (TU Delft) Joana van Nieuwkoop	

# Summary

During storm conditions infragravity (IG) waves significantly affect runup and potential overtopping of dikes with shallow foreshores. However, it is unclear how much impact these IG waves will have on the potential flooding due to failure of the Dutch flood defences during normative conditions. Initial explorations suggest that they can be significant but with a wide range in uncertainty. Currently, the presence of IG waves is not included in the instrumentation that is used to assess the safety level of flood defences, the so-called “Beoordelings- en Ontwerp instrumentarium” (BOI), introducing uncertainty in the determination of flood probability. The uncertainty is particularly large in the shallow Eastern Wadden Sea and the entrance of the estuaries of the Eastern Scheldt and Western Scheldt.

The range of IG waves on the shallow foreshores in front of Frisian and Groningen dikes and their effect on the failure probability of these dikes has been estimated. Use has been made of available SWASH hindcasts of the November 2007 storm and an extreme scenario in which the water level of that was increased by two meters. The IG wave height showed a clear evolution from offshore to the ebb-tidal delta, where IG waves that were bound to the sea-swell at the North Sea were released, and propagated towards the dike, gradually losing some energy. Apart from the sea swell component free IG waves reach the Wadden Sea, arriving from adjacent and distant coasts. The free IG wave height offshore was determined by extreme value analysis by TU Delft (2025) and translated from the ebb-tidal delta to the dike assuming the same evolution as the sea-swell component. Both IG component are of the same order. For the extreme case the total IG wave height varies between 0.4 and 0.9 m.

For this case the effect on the wave runup height  $z_{2\%}$  is 0.8 - 2 m. The failure probabilities for the mechanisms GEKB and GEBU-Golfklap increase with a factor in the range of 1.5-2 and 2-5 respectively, which can be considered as a lower boundary for the more extreme cases. For the storm hindcast and the extreme scenario the same offshore wave boundary conditions were imposed. If offshore wave boundary conditions, including IG waves, would have been considered that were consistent with the extreme water level considered, the failure probabilities for both mechanisms would have been larger. For the less sheltered eastern part of the Wadden Sea, the Eems-Dollard excluded, the IG wave heights are likely to be of the same order. The same holds for the IG wave heights in front of the Eastern Scheldt barrier, in the Western Scheldt they are probably smaller.

The uncertainty in the effect of including IG waves on the failure probability has been reduced. It can be concluded that IG waves do have a significant effect. It is recommended to implement IG waves in BOI, so that a more realistic estimate of the run-up and overtopping of dikes is obtained.

# Content

	<b>Summary</b>	<b>4</b>
	<b>Content</b>	<b>5</b>
<b>1</b>	<b>Introduction</b>	<b>7</b>
1.1	Background	7
1.2	Objective	7
1.3	Overall approach and reader's guide	7
<b>2</b>	<b>Release of bound IG waves</b>	<b>9</b>
2.1	Available SWASH results	9
2.2	Extracting wave conditions at the toe of the dike	10
2.2.1	Lauwersgat	10
2.2.2	Frisian Inlet	12
2.3	Accounting for dike reflection	13
2.3.1	Lauwersgat	13
2.3.2	Frisian inlet	15
2.4	Conditions with increased water level	16
2.4.1	Wave heights	16
2.4.2	Spectral shape	18
<b>3</b>	<b>Remote free IG waves</b>	<b>19</b>
3.1	FIG boundary conditions	19
3.2	Wave height transformation and spectral shape	19
<b>4</b>	<b>Locally generated bound IG waves</b>	<b>22</b>
4.1	SWAN model set-up	22
4.2	Wind sea conditions in the Wadden Sea	22
4.2.1	Lauwersgat	22
4.2.2	Frisian inlet	24
4.3	BIG waves from locally generated wind waves	25
4.3.1	Lauwersgat	25
4.3.2	Frisian inlet	26
<b>5</b>	<b>Analysis of total IG wave energy</b>	<b>28</b>
5.1	Evolution of remote and locally generated IG waves	28
5.2	Bandwidth IG waves	30
<b>6</b>	<b>Estimate of impact on flood probability</b>	<b>32</b>
6.1	Effect of IG waves on wave run up.	32
6.2	Analysis of the impact of including IG waves	32

6.3	Discussion	33
7	<b>Conclusions</b>	<b>34</b>
8	<b>References</b>	<b>35</b>
A	<b>Effect of IG waves on dike erosion</b>	<b>36</b>

# 1 Introduction

## 1.1 Background

Infragravity (IG) waves are known to affect wave runup and overtopping of dikes with shallow foreshores (e.g., Van Gent, 2001; Lashley et al., 2020). Despite this, IG waves are currently not explicitly included in the instrumentation that is used to assess the safety level of Dutch flood defences, the so-called “Beoordelings- en Ontwerp instrumentarium” (BOI). This omission introduces a potential uncertainty in the national assessment of the flood probability of coastal dikes.

Currently, it is not clear to what extent IG waves affect potential overtopping and flooding of the Dutch coastal dike flood defences during normative conditions. This uncertainty is particularly large in the shallow Eastern Wadden Sea, where the IG wave height reaching the dikes along the coast of Friesland and Groningen during extreme conditions is largely unknown. This uncertainty is composed of two aspects. The first is related to the unknown penetration of IG waves resulting from sea-swell forcing at the ebb-tidal delta (release of bound IG waves). The second is related to the penetration of IG waves arriving from adjacent and distant coasts. For the estimation of these remote free IG waves we make use of a concurrent study (TU Delft, 2025) into the influence of free IG waves on dune erosion during extreme conditions.

The study has been carried out in the framework of the Dutch research program ‘Kennis voor Keringen’ (KvK, translation: Knowledge for Flood Defences). The KvK program is tasked to develop knowledge to support the safety assessment and design of primary flood defences in the Netherlands. As part of the KvK research program, Deltares and Rijkswaterstaat aim to gain understanding of the importance of IG wave processes affecting the flood probability estimates in the Netherlands.

## 1.2 Objective

The objective of this research is to reduce the range of uncertainty relating to the impact of the inclusion of IG waves heights on flood probability estimates. To this end, this research focusses on sea dikes with shallow foreshores along the Dutch Eastern Wadden Sea coast, as well as the entrance of the Eastern and Western Scheldt estuaries, where estimates of IG wave heights are most uncertain. Specifically, this research aims to quantify the range of IG conditions on the shallow foreshores in front of sea dike in Friesland and Groningen, and estimate the effect of IG waves on the failure probability of these dikes. Results for this region are subsequently translated to the entrance of the estuary of the Eastern Scheldt and the Western Scheldt.

## 1.3 Overall approach and reader’s guide

As mentioned in Section 1.2, both the range of IG waves on the shallow foreshores in front of Frisian and Groninger dikes will be estimated, as well as their effect on the failure probability. This is achieved by combining information on (released) bound IG waves and free IG waves, as well as their effect on predicted wave runup and overtopping. Steps applied in this analysis are described below.

In this study the models SWASH and SWAN have been applied to estimate the bound (released) IG waves generated by sea-swell at the North Sea and locally inside the Wadden Sea respectively. The phase-resolving model SWASH is able to accurately predict the

evolution of the bound IG waves that are imposed at the offshore model boundary. The model does not include wind generation. Therefore, also the phase-averaged wave model SWAN has been used. Since offshore boundary conditions have not been imposed, SWAN determines only the locally generated wind sea. SWAN does not compute the bound IG wave created by the locally generated wind sea. Therefore, a postprocessing step is required to determine the bound IG wave energy, which is summed to the IG wave energy determined by SWASH, the FIG and wind-sea energy determined by SWAN. Here we assume that the effect of nonlinear interactions between wind sea, bound IG waves and released bound IG waves can be neglected. For this study this assumption seems reasonable.

The release of bound IG waves is considered in Chapter 2. For the storm of 8 and 9 November 2007, a hindcast is made with the phase resolving wave model SWASH in Van Rijnsdorp et al. (2023) for two regions in the eastern part of the Wadden Sea, i.e. the Frisian Inlet and Lauwersgat. The results include bound IG waves that were released on the ebb-tidal delta and propagate into the Wadden Sea. Results of the same storm are available but with a 2 m increased water level. SWAN computations are carried out for the same storms to provide energy density spectra of locally generated wind sea.

The contribution of free (remote) IG waves are estimated qualitatively in Chapter 3. These results are based on research in a concurrent KvK project. Coincident bound IG wave energy in the Wadden Sea, relating to the local wind sea conditions computed by SWAN, are estimated in Chapter 4 using Hasselmann's (1962) formulae.

The evolution from the offshore ebb-tidal delta to nearshore locations along the dikes of the combined free IG and (released) bound IG wave spectra is analysed in Chapter 5. Conclusions from the analyses for the Wadden Sea are subsequently generalized to other coastal regions.

Chapter 6 presents a re-evaluation of the impact of IG waves on wave run-up and overtopping based on the updated estimate of IG wave conditions derived in this study and existing empirical runup and overtopping equations. Final conclusions are presented in Chapter 7.

## 2 Release of bound IG waves

The analysis of (released) bound IG waves is based on available SWASH simulations of the November 2007 storm and a more extreme case with a 2 m increased sea level (SLR). The available SWASH simulations are described in Section 2.1. In Section 2.2 a proxy for the IG wave height at the toe of the dike is determined. For the more extreme scenario, only the simulation with the sponge layer<sup>1</sup> is available, without the presence of the dike. This sponge layer is located approximately 5 km offshore of the dike location. To assess the effect of the presence of the dike on the wave conditions at the toe, an inter-comparison is made for the 2007 (without SLR) storm simulations with the dike and the sponge layer, see Section 2.3. In Section 2.4 this effect is then incorporated in the translation of the wave conditions at the sponge layer for the scenario with the SLR.

### 2.1 Available SWASH results

As part of an earlier study on the low-frequency wave penetration into the Eastern Waddenzee, SWASH simulations were performed as a benchmark for subsequent SWAN predictions (Rijnsdorp et al., 2023, Deltares, 2024). Low-frequency in this case refers to the low-frequency tail of the sea-swell waves (0.03 Hz-0.2 Hz). More specifically, SWASH was used to hindcast the storm of November 2007 during which penetration of low-frequency storm waves has been observed. This was done for two domains, i.e., the Frisian Inlet and Lauwersgat (see Figure 2.1). These computations were performed with and without the presence of the dike. The potential effect of sea level rise (SLR) was explored by raising the storm surge level of the storm (set at NAP+3 m<sup>2</sup>) by an additional 2 m, resulting in a total surge level of NAP+5 m. As such, the latter can be considered as representative for more extreme storm conditions (with a return period of 10,000 years), although it must be kept in mind that the wave forcing was not increased accordingly. The raised water level simulation was only successfully carried out for the Lauwersgat model domain without the presence of the dike (only sponge layer). The availability of SWASH simulations is summarized in Table 2.1.

*Table 2.1 Availability of SWASH simulations with the presence of a dike or sponge layer for the 2007 storm without and with 2m Sea Level Rise (A and N/A are available and not available respectively). For the simulations including the dike, only the total wave height is available. For the simulations with the sponge layer, time series of the surface elevation are available to separate the IG waves.*

Domain	dike	Sponge	dike+SLR (2m)	Sponge+SLR (2m)
Friesche zeegat	A	A	N/A	N/A
Lauwersgat	A	A	N/A	A

SWASH is a non-hydrostatic intra-wave model that resolves the evolution of a directionally spread wave field over a variable bathymetry including wave breaking, bed friction and non-linear interactions that shape the wave surface elevation. The offshore boundary condition for the SWASH simulations is a time series of the incident waves based on the wave-buoy measured spectrum at SON to which the bound IG waves are added, as these are not

<sup>1</sup> A sponge layer is a down-wave (a few kilometres from the dike) boundary condition of the SWASH model that absorbs the incoming wave energy.

<sup>2</sup> The maximum water level measured at Lauwersoog is approximately NAP + 3.5 m, having a return period of approximately 30 years. The imposed water level in the SWASH computations for both Lauwersgat and Friesche Zeegat is NAP + 3m.

measured by the wave buoy. Given the fact that the SWASH simulations include the full IG range, defined in this report as (0.004 Hz-0.04 Hz), it provides an opportunity to explore the penetration and transformation of sea-swell forced IG waves from offshore, to a location near the toe of the dike, during these more extreme conditions. To this end, model time series have been used to separate the wind waves ( $f > 0.04$  Hz) from the IG waves within the SWASH domain. As a first step, the influence of the wave reflection by the dike has been examined by intercomparing the IG and sea-swell wave height at a fixed nearshore transect with and without the presence of the dike. Next, the IG and sea-swell wave height for the case with increased SLR have been examined and corrected for the presence of the dike taking the estimated reflection into account.

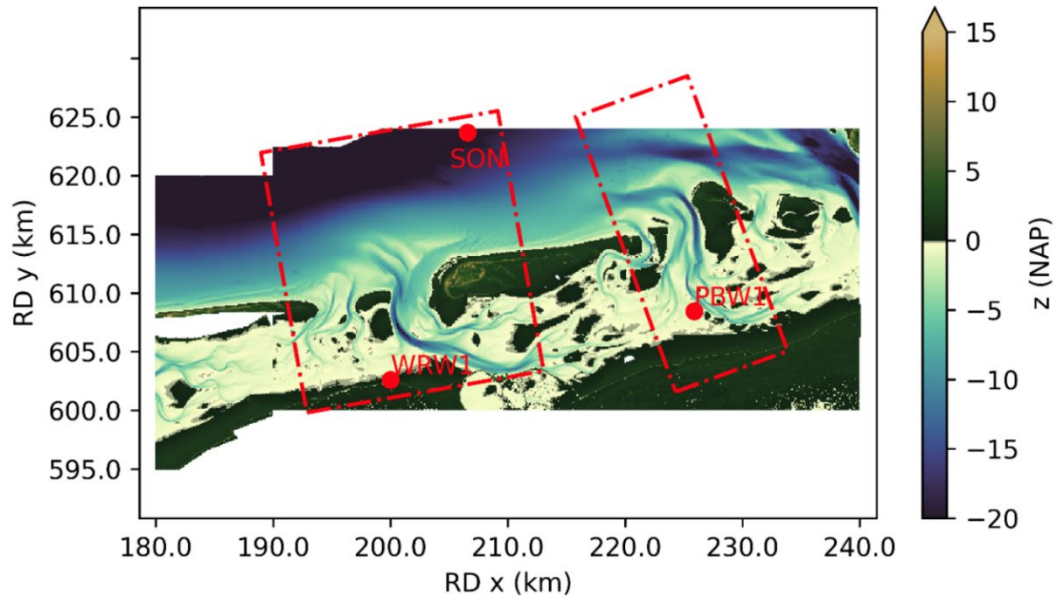


Figure 2.1 Overview of the bathymetry (based on vaklodigen and AHN data) near the Frisian inlet and Lauwersgat. The red markers indicate the available measurement stations in this region of interest, and the red rectangles indicate the two inlets that were modelled in this study with on the left the Frisian Inlet and on the right the Lauwersgat (Figure 49 from Rijnsdorp et al., 2023).

## 2.2 Extracting wave conditions at the toe of the dike

The stored time series of the SWASH computations (Rijnsdorp et al., 2023) do not include the toe of the dike. However, the spatial distribution of the total wave height, i.e. the combined sea-swell and IG, has been stored. This can be used to explore the transformation of the conditions at a reference line a few kilometres offshore of the dike, to the toe of the dike. The reference line is located just prior to the sponge layer used in the model simulations without the presence of the dike (see Rijnsdorp et al., 2023 for details).

### 2.2.1 Lauwersgat

The spatial distribution of the total significant wave height, made up of the combined sea-swell and IG wave heights, for the Lauwersgat in the presence of the dike is shown in the left panel of Figure 2.2. The corresponding bathymetry is shown in the panel on the right. There is a strong decay in wave height over the ebb-tidal delta and the wave penetration towards the coast is clearly affected by the presence of the tidal channels.

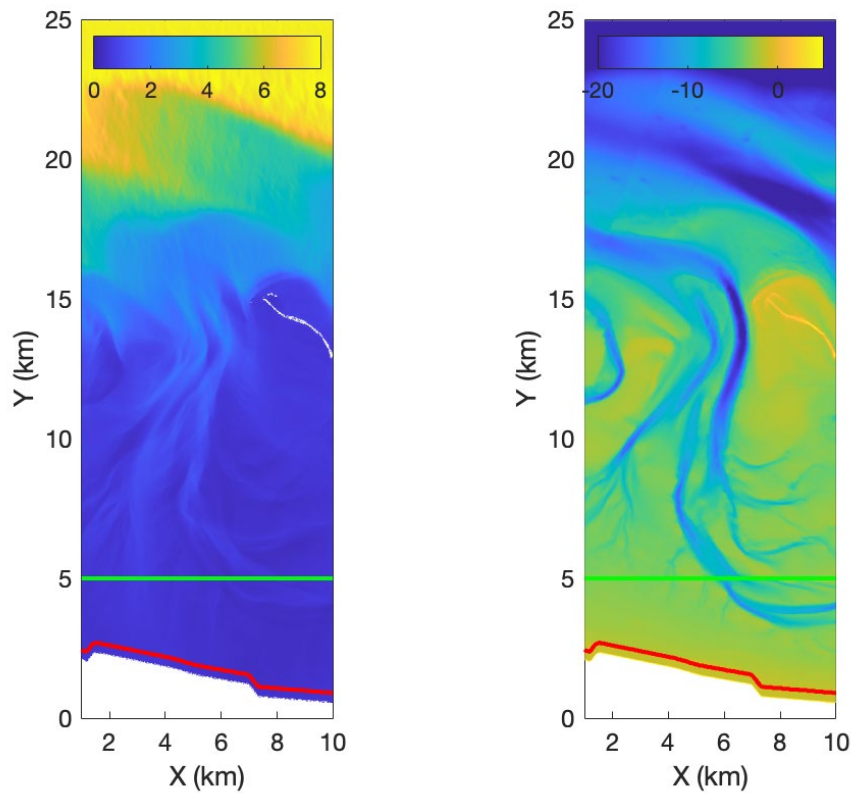


Figure 2.2 Significant wave height (left panel) and corresponding bathymetry (right panel) during the November 2007 storm condition for the Lauwersgat. The colour scales are in m. Location of the dike toe and the reference transect are given by the red and green line respectively.

The output of the total wave height at the approximate location of the toe of the dike is compared with the nearshore reference transect in the left panel of Figure 2.3. This shows that in the transformation of the wave height from the reference transect to the toe of the dike, the wave height distribution becomes smoother, but the overall wave height stays more or less the same (compare box plots in the right panel of Figure 2.3) even though there is significant bathymetric variability in between the toe and the reference line (see right panel of Figure 2.2). The results suggest that the wave height at the reference line can be used as a proxy for the wave height at the toe of the dike.

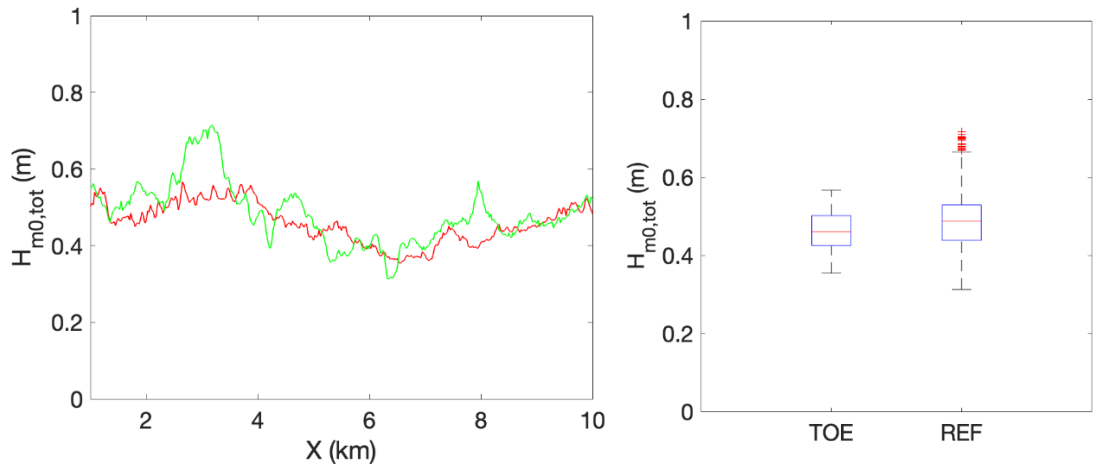


Figure 2.3 Left panel: Comparison of the total significant wave height along the toe of the dike (red) and the reference transect (green) for the 2007 storm condition in the Lauwersgat. Right panel: Box plot of the combined significant wave height along the dike toe (TOE) and the reference transect (REF). Red horizontal lines refer to the median value and the bottom and top of the box to the 25 and 75 percentiles respectively.

## 2.2.2 Frisian Inlet

Performing the same analysis for the Frisian Inlet the total significant wave height and the corresponding bathymetry are shown in Figure 2.4. The output of the total wave height at the approximate location of the toe of the dike is again compared with the nearshore reference transect in the left panel of Figure 2.5. In this case there is clearly an alongshore gradient in the wave height along the dike with the highest waves on the western part and the smallest waves at the eastern side coinciding with the location of Ameland (see right panel in Figure 2.4). Both the median and the variability are of similar order (see right panel of Figure 2.5).

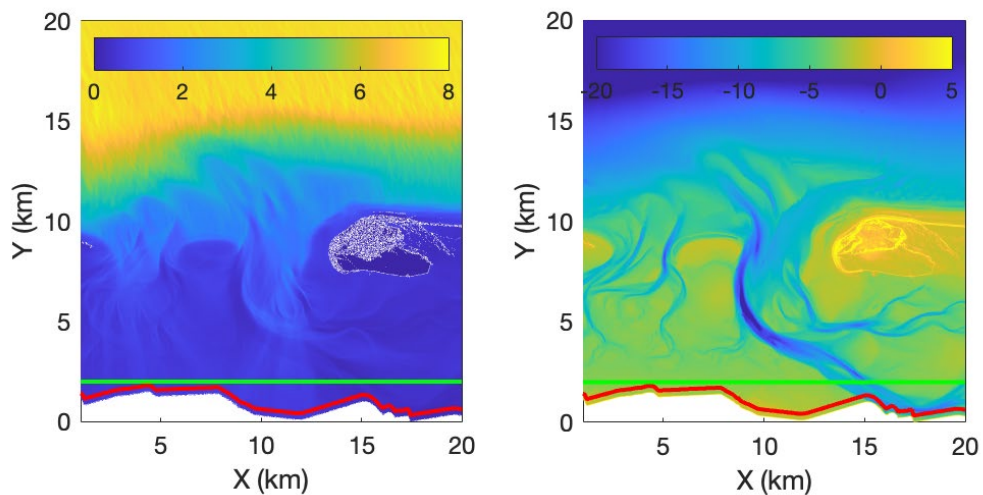


Figure 2.4 Total significant wave height (left panel) and corresponding bathymetry (right panel) during the 2007 storm condition for the Frisian inlet. The color scale is in m. Location of the dike toe and the reference transect are given by the red and green line respectively.

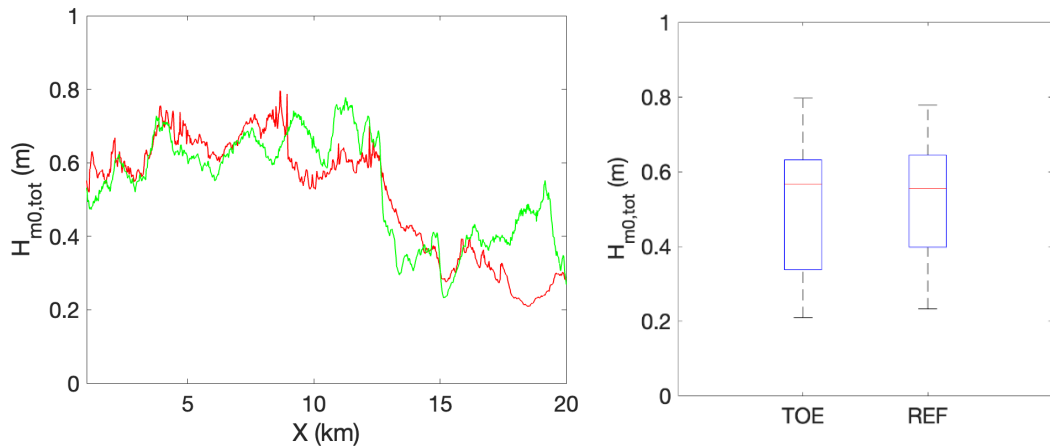


Figure 2.5 Left panel: Comparison of the total significant wave height along the toe of the dike (red) and the reference transect (green) for the 2007 storm condition in the Frisian Inlet. Right panel: Box plot of the combined significant wave height along the dike toe (TOE) and the reference (REF) transect. Red horizontal lines refer to the median value and the bottom and top of the box to the 25 and 75 percentiles respectively.

The results at both locations suggest that a reference line close to the dike just offshore of the sponge layer can indeed be used as proxy for the conditions at the toe of the dike. The subsequent analyses of the SWASH timeseries will be based on these reference lines, starting with the role of reflections.

## 2.3 Accounting for dike reflection

The presence of the dike in the SWASH model will result in reflections of the incident waves. The reflection process is resolved within the model, i.e. reflection coefficients are not used, and depends on the steepness of the incident waves, the slope of the dike and the incidence angle. It is expected that, due to limitations in model resolution, the model will provide conservative values of reflection (i.e., close to fully reflective). In the following, the sea-swell and IG wave heights are examined at the respective reference lines discussed above, with and without the presence of the dike. The objective is to see whether it is possible to correct the wave heights obtained without the presence of the dike to match the results obtained in the presence of the dike. This is important in the interpretation of the results for the extreme case with increased surge level that are only available without the presence of the dike.

### 2.3.1 Lauwersgat

The shoaling of the sea-swell results in a strong increase of the forced IG waves at the offshore boundary (see Figure 2.6). Within the breaker zone on the outer delta, indicated by the rapid decrease in the significant wave height of the sea-swell (left panel, the zone located in between  $Y=18$  and  $Y=23$  km) the significant IG wave height is more or less constant (right panel, the zone located in between  $Y=18$  and  $Y=23$  km), suggesting that the transfer of energy from the sea-swell to the IG waves is weak. These released IG waves subsequently propagate freely towards the coast with higher IG wave heights on the flats in between the tidal channels.

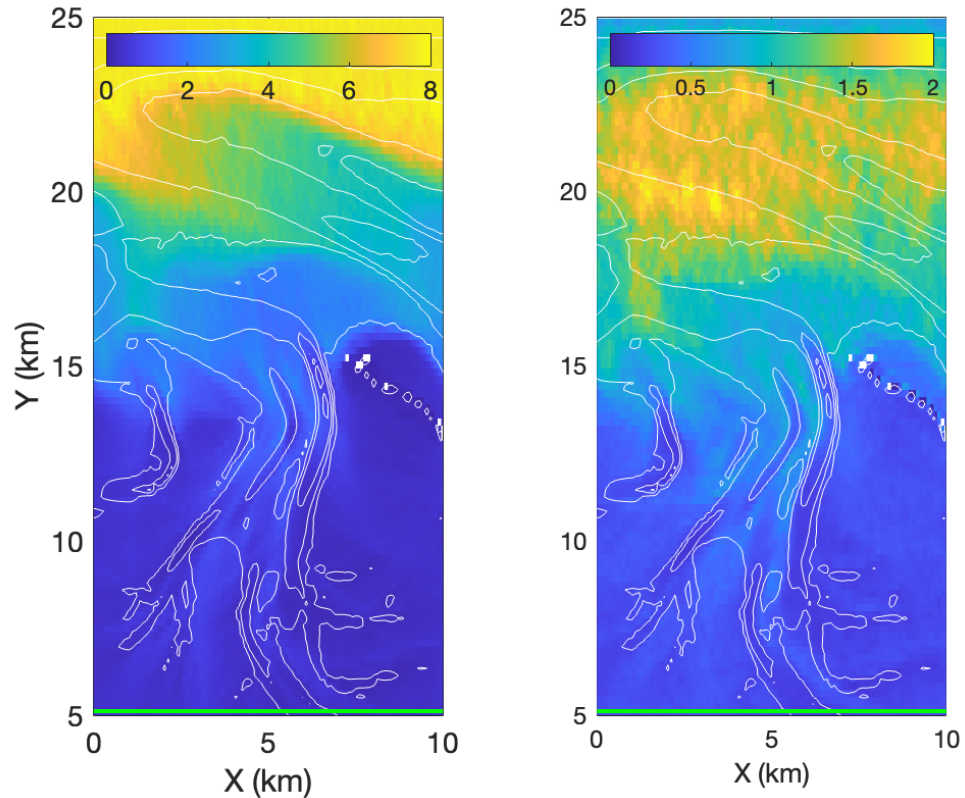


Figure 2.6 Significant sea-swell wave height (left panel) and corresponding IG wave height (right panel) during the November 2007 storm condition for the Lauwersgat in the presence of the dike. The colour scale is in m (note the difference in scales). Location of the reference transect is given by the green line at the bottom.

Examining the significant wave height at the reference line shows that the predictions without the presence of the dike are significantly lower than when the dike is included. This holds for both the sea-swell and IG wave heights (compare blue and green lines in the left panels of Figure 2.7). Assuming full reflection of both the sea-swell and IG wave heights,  $H_{m0,reflected} = H_{m0,nodike}$ , to estimate the total significant wave height:

$$H_{m0,tot} = \sqrt{H_{m0,nodike}^2 + H_{m0,reflected}^2}$$

shows a reasonable match with the results including the dike, although local differences are apparent around  $X = 8$  km. This mismatch corresponds to the location where there is a sudden change in the orientation of the dike (see Figure 2.2), thereby affecting the reflection. Furthermore, potential phase coupling between the incident and reflected waves have been ignored. Overall, the alongshore variability is well represented by assuming full reflection as can be inferred from the box plots with a minor underestimation of a few centimetres of the median IG wave height, being  $O(0.25$  m) (see right panels in Figure 2.7).

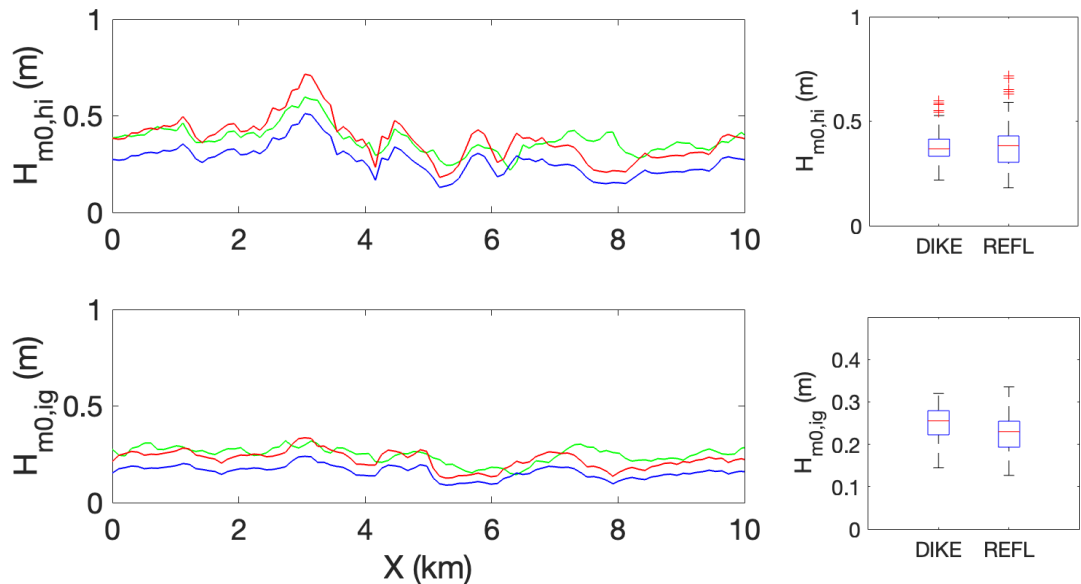


Figure 2.7 Upper left panel: Significant sea-swell wave height at the reference line with dike (green line), without the dike (blue line) and assuming full reflection (red line). Lower left panel: The same for the IG wave height. Upper right panel: Box plot of the combined sea-swell wave height along the reference transects with dike (DIKE) and without the dike but with full reflection (REFL). Red horizontal lines refer to the median value and the bottom and top of the box to the 25 and 75 percentiles respectively. Lower right panel: The same for the IG wave height.

### 2.3.2 Frisian inlet

Performing the same analysis for the Frisian inlet shows the sheltering effect of the Wadden islands Ameland and Terschelling reducing the wind sea wave height along the dike in the eastern and western end of the inlet (see left panel of Figure 2.8). The IG waves are more diffuse due to their larger directional spreading (see right panel of Figure 2.8) compared to the sea-swell waves. Similarly to the case of the Lauwersgat, an initial increase in IG wave height is observed in the shoaling zone which stays more or less constant within the outer surf zone. There is a decrease in the IG wave height in the inner surfzone over the ebb tidal shoals (zone located between  $Y = 10$  and  $12$  km), potentially related to recurrence (Rijnsdorp et al., 2024). Once released, the IG waves propagate into the inlet towards the dike where the interaction with the channels and shoals is evident, but also towards the lee side of for instance Ameland.

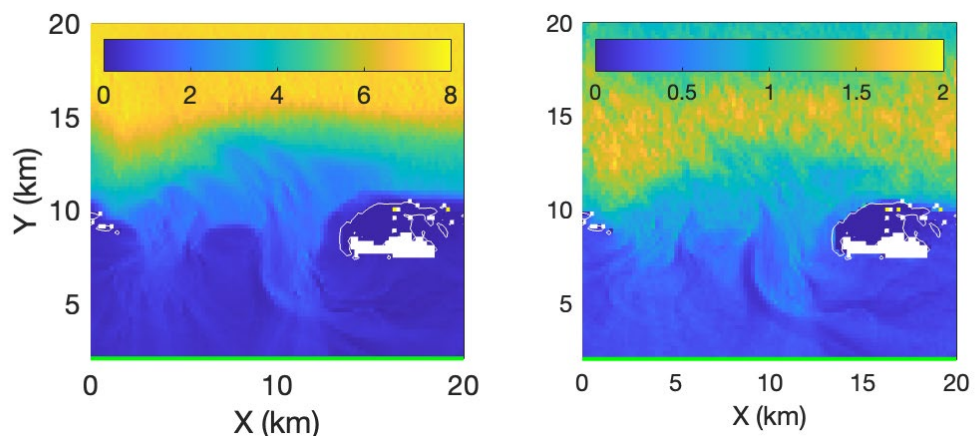


Figure 2.8 Significant sea-swell wave height (left panel) and corresponding IG wave height (right panel) during the 2007 storm condition for the Frisian inlet including the dike. The colour scale is in m (note the difference in scales). Reference transect is given by the green line at the bottom.

Comparing the sea-swell wave height at the reference line shows significant variability alongshore (see left panel of Figure 2.9) consistent with the earlier mentioned sheltering effect by the Wadden islands (see left panel of Figure 2.8). Taking the results from the computation without the dike and assuming full reflection of the sea-swell waves gives a good match with the results obtained in the presence of the dike. This is further supported by comparing the sea-swell wave height distribution along the reference line (see right upper panel in Figure 2.9).

The IG waves show significantly less variability along the reference line, although some of the sheltering by the Wadden islands is evident (see lower left panel of Figure 2.9). Assuming full reflection of the incident IG waves predicted without the dike shows again a good match with the results obtained with the dike included, with median values of  $O(0.25)$  m.

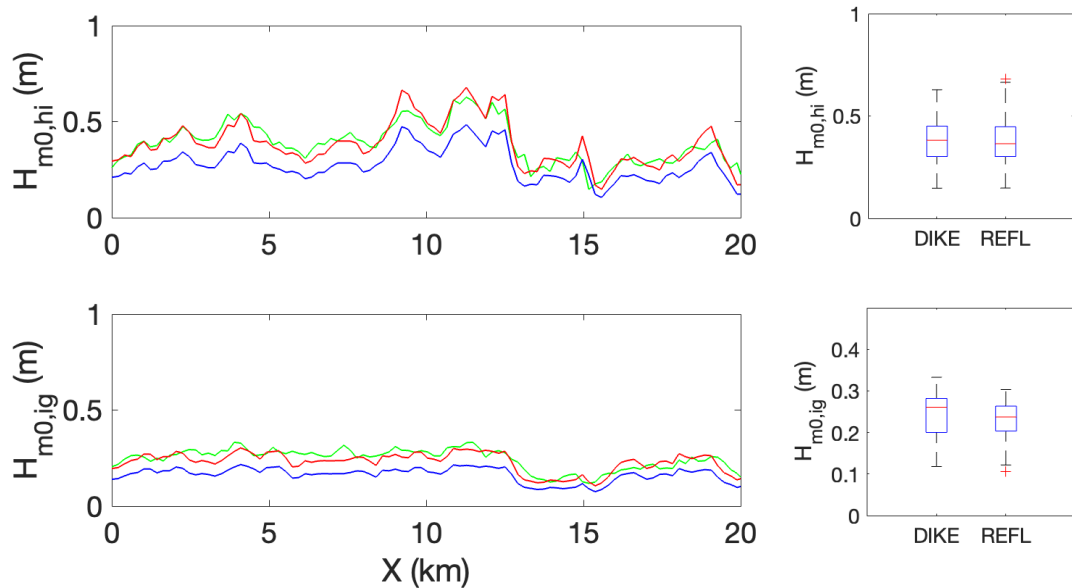


Figure 2.9 Upper left panel: Significant sea-swell wave height at the reference line with dike (green line), without the dike (blue line) and assuming full reflection (red line). Lower left panel: The same for the IG wave height. Upper right panel: Box plot of the combined sea-swell wave height along the reference transects with dike (DIKE) and without the dike but with full reflection (REFL). Red horizontal lines refer to the median value and the bottom and top of the box to the 25 and 75 percentiles respectively. Lower right panel: The same for the IG wave height.

## 2.4 Conditions with increased water level

### 2.4.1 Wave heights

For the case of the Lauwersgat, the mean sea level during the November 2007 storm was raised by another 2 m to account for future sea level rise, thus resulting in a 5 m sea level offset. Here we use the results of the NAP + 5 m simulation to get insight in the potential increase in the sea-swell and IG wave heights during extreme storm. Given the fact that the incident sea-swell wave height has not been changed, the offshore conditions are similar to the case without the additional 2 m water level offset (compare left panels of Figure 2.10 and Figure 2.6). Inside the domain, the onset of wave breaking is delayed and more of the sea-swell energy is propagating through the inlet towards the dike section. The maximum IG wave height located on the outer delta is similar in magnitude as in the case without the additional 2 m water level offset (compare right panels in Figure 2.10 and Figure 2.6), but slightly displaced in the onshore direction. The increased water level clearly facilitates the penetration of IG waves into the inlet towards the dike section (Figure 2.11). Both the sea-swell wave height and the IG wave height are more than double compared to the conditions

without the 2 m increase in water level along the reference line close to the dike, compare Figures 2.7 and 2.11.

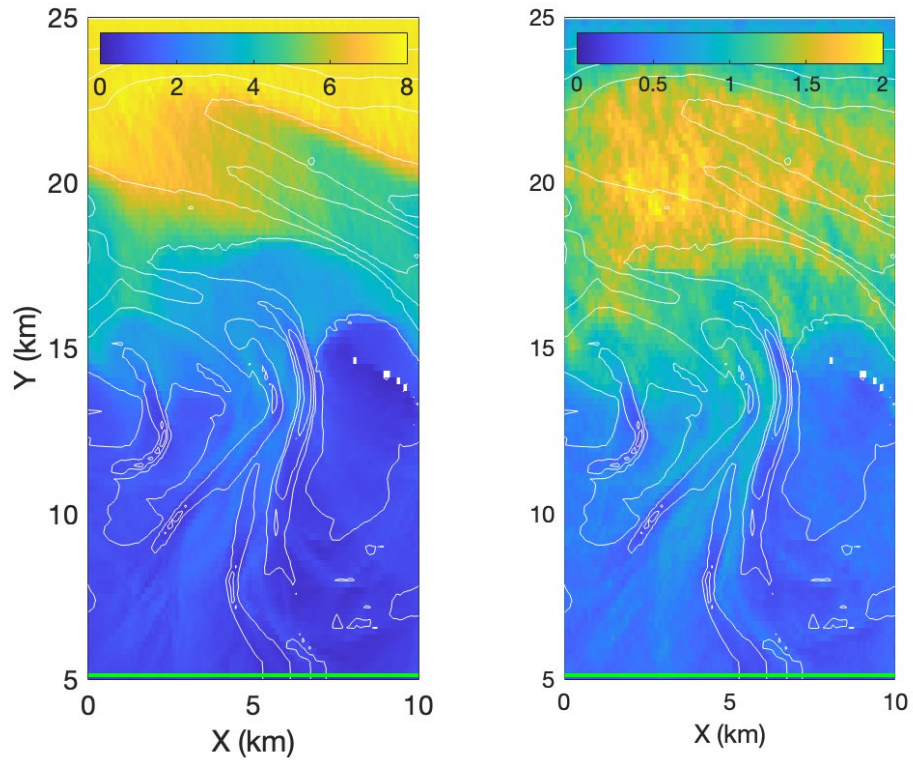


Figure 2.10 Significant sea-swell wave height (left panel) and corresponding IG wave height (right panel) during the 2007 storm condition with an additional 2 m sea level increase for the Lauwersgat without the presence of the dike. The colour scale is in m (note the difference in scales). Location of the reference transect is given by the green line at the bottom.

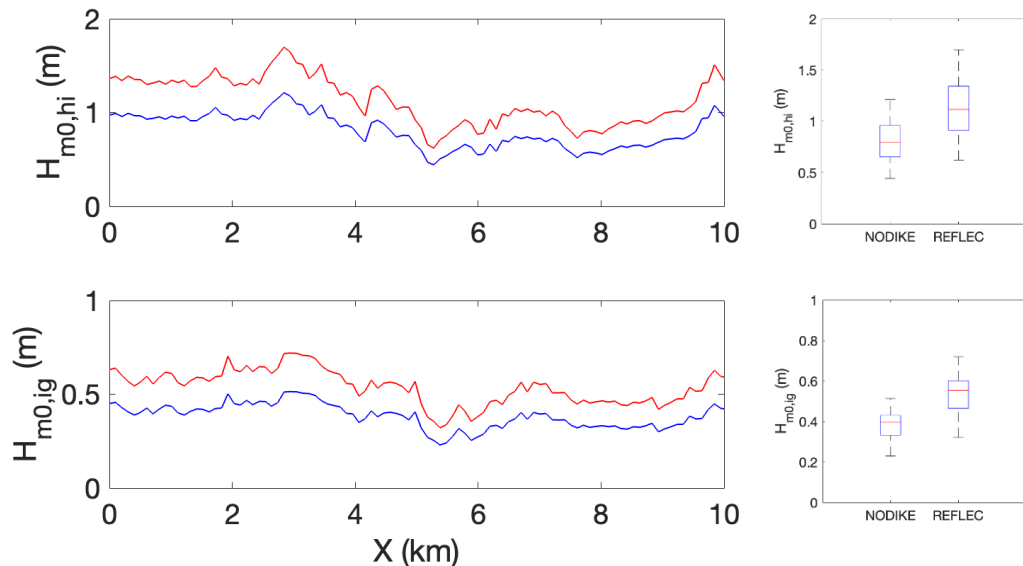


Figure 2.11 Upper left panel: Significant sea-swell wave height at the reference line without the dike (blue line) and assuming full reflection (red line) for a 2m increase in the mean water level. Lower left panel: The same for the IG wave height. Upper right panel: Box plot of the combined sea-swell wave height along the reference transect without dike (NODIKE) and without the dike but with full reflection (REFLEC). Red horizontal lines refer to the median value and the bottom and top of the box to the 25 and 75 percentiles respectively. Lower right panel: The same for the IG wave height.

### 2.4.2 Spectral shape

The spectral shape of the incident sea-swell and IG waves is examined next for the case with the increased water level as this contributes to the potential runup and overtopping. The frequency spectrum along the reference line ( $Y = 5$  km), considered to be representative for the incoming waves at the toe of the dike, is shown in the top panel of Figure 2.12. Individual spectra are somewhat grassy due to the limited degrees of freedom (75 d.o.f.), but the patterns are consistent with the alongshore variability that is observed in the sea-swell and IG wave heights (see Figure 2.11). The alongshore averaged spectrum shows a smooth transition between the IG and sea-swell conditions, i.e. there is not a clear separation between the IG and sea-swell energy density distribution that was present at the offshore boundary (not shown).

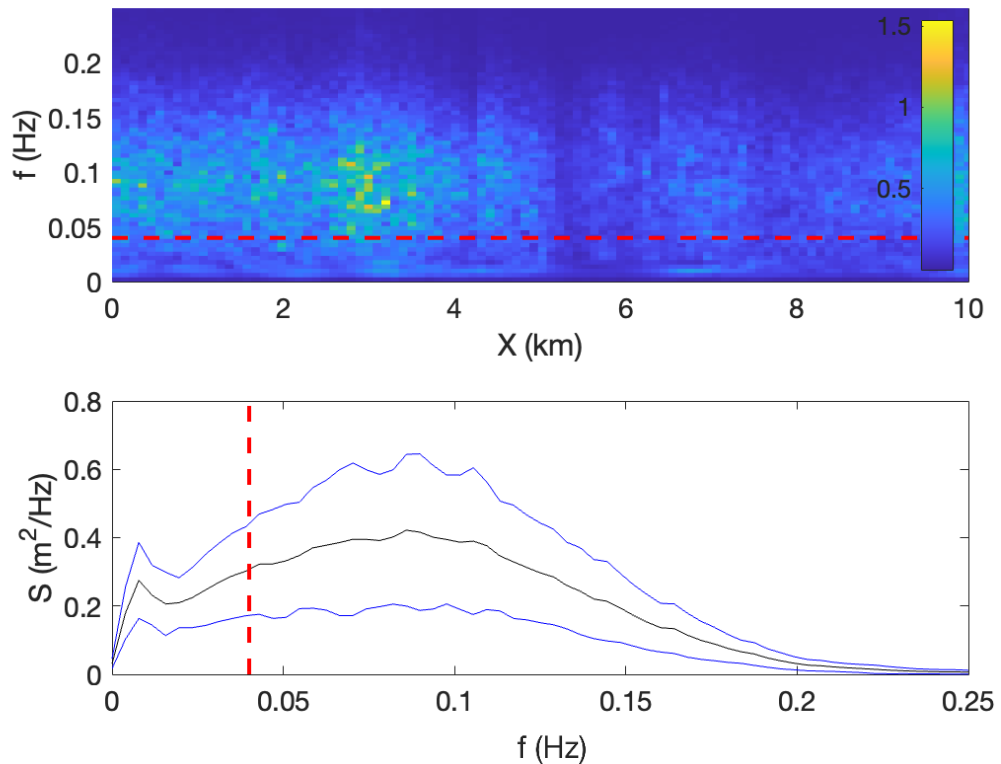


Figure 2.12 Top panel: Frequency spectrum along  $Y = 5$  km (representative for the expected incident conditions at the toe of the dike) with energy density in  $\text{m}^2/\text{Hz}$  expressed by the colour bar. Bottom panel: Alongshore averaged surface elevation spectrum (black line) plus or minus the standard deviation (blue dashed lines). The delineation between sea-swell and IG waves is given by the red dashed lines in both panels.

### 3 Remote free IG waves

For the estimation of remote free IG waves we make use of a concurrent KvK study (TU Delft, 2025) into the influence of free IG (FIG) waves on dune erosion during extreme conditions. This will provide an estimate of the incident FIG waves at the outer model boundary. Using the SWASH model predictions, we will estimate the potential contribution of these FIG waves along the dike using the 2007 storm as a template. Adding both contributions will give a first estimate of the range in expected IG wave heights at the toe of the dike during extreme storm conditions.

#### 3.1 FIG boundary conditions

The incident FIG wave height from remote beaches needs to be added to the locally released IG waves obtained from the SWASH simulations at the toe of the dike. The offshore boundary condition for the incident FIG wave height is obtained from the 40+ year SWAN-FIG hindcast described in the report on the impact assessment of incident FIG waves on dune erosion during extreme conditions along the Dutch coast (TU Delft, 2025). Using a Gumbel distribution to plot the yearly maximum incident FIG wave heights, the expected 10,000 year return period incident FIG wave height is 0.58 m at 25 m water depth.

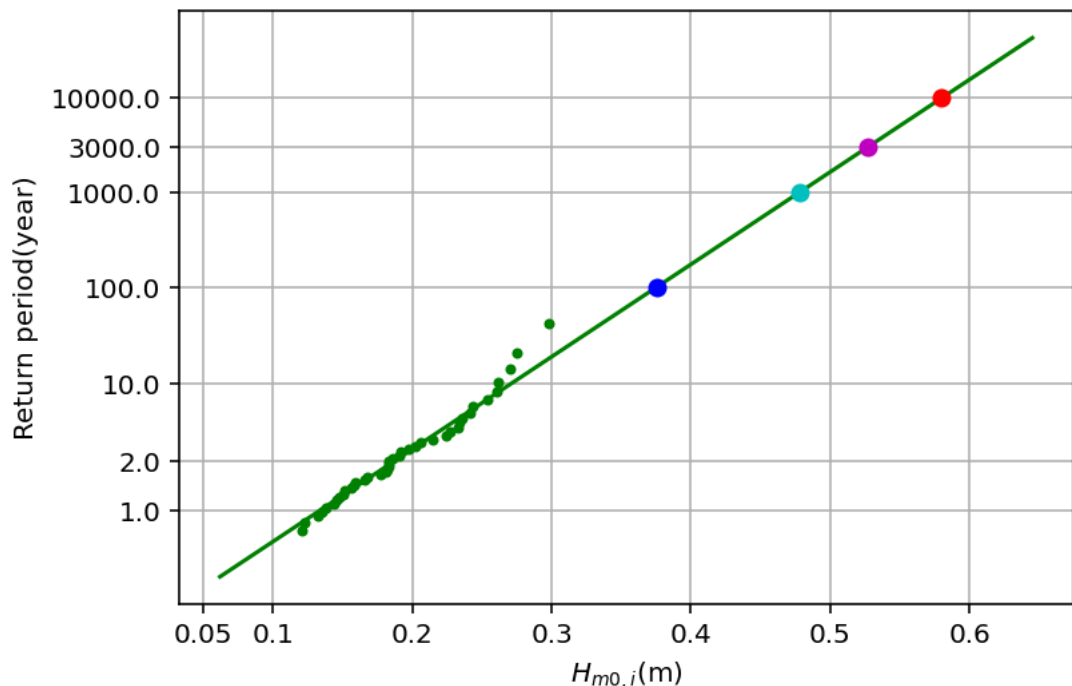


Figure 3.1 Yearly maxima for the Eastern Wadden Sea obtained from the SWAN-FIG hindcast over 40+ years at 25 m water depth plotted on a Gumbel scale. The 1/100 (blue), 1/1000 (cyan), 1/3000 (purple) and 1/10000 (red) return periods are given by the coloured dots.

#### 3.2 Wave height transformation and spectral shape

The incident FIG wave height is shoaled to the alongshore transect Y = 18 km that is located offshore from the channel and shoals within the inlet and where the locally generated IG waves obtained from the SWASH simulation are all released (see left panel of Figure 3.2):

$$H_{m0,FIG}(X, Y)_{Y \geq 18 \text{ km}} = H_{m0,FIG,1/10000} \left( \frac{25}{d(X, Y)_{Y \geq 18 \text{ km}}} \right)^{0.7}$$

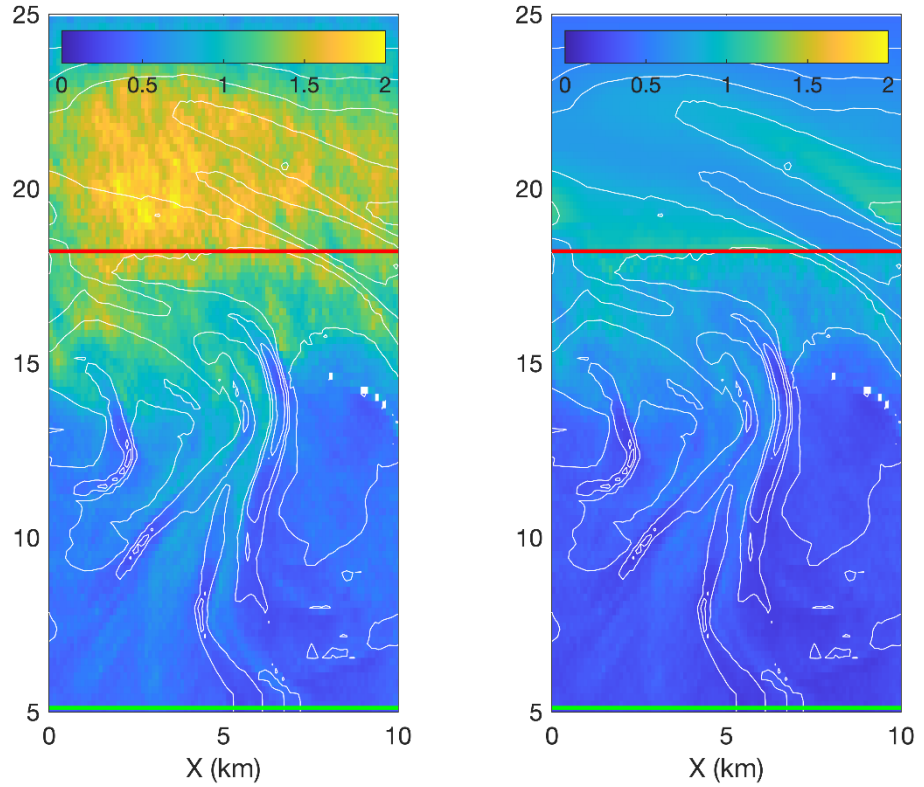


Figure 3.2 Left panel: Significant IG wave height (right panel) during the 2007 storm condition with an additional 2 m sea level increase for the Lauwersgat without the presence of the dike obtained from the SWASH simulation. Right panel: Incident FIG wave height. The colour scale is in m. Location of the reference transect is given by the green line at the bottom. The location for the FIG wave transformation is given by the red line.

The shoaling parameter of 0.7 is representative of a directionally broad IG wave field including refractive trapping and was obtained from a comparison of the IG wave heights at 25 m and 20 m depth in the study by TU Delft [2025].

Next, the wave transformation of the released IG waves in SWASH is used to scale the FIG wave transformation towards the reference line near the toe of the dike:

$$H_{m0,FIG}(X, Y)_{Y < 18 \text{ km}} = H_{m0,IG}(X, Y)_{Y < 18 \text{ km}} \frac{\overline{H_{m0,FIG}(X, Y)_{Y=18 \text{ km}}}}{\overline{H_{m0,IG}(X, Y)_{Y=18 \text{ km}}}}$$

The combined FIG wave height is shown in the right panel of Figure 3.2. The FIG wave height at the reference line can now be added to the SWASH result assuming full reflection (leading to the factors 2, as explained in Section 2.3.1):

$$H_{m0,IG,tot,Y=5km} = \sqrt{2H_{m0,IG,Y=5km}^2 + 2H_{m0,FIG,Y=5km}^2}$$

to obtain the combined wave height of FIG and released IG waves from offshore (see Figure 3.3). This combined wave height is 0.6 – 0.9 m, with slightly smaller values in the channel (5 km < X < 6 km). Adding the spectral density of the incident FIG waves to the

SWASH spectrum leads to an increase in the IG frequency band (compare lower panels of Figure 2.12 and Figure 3.3).

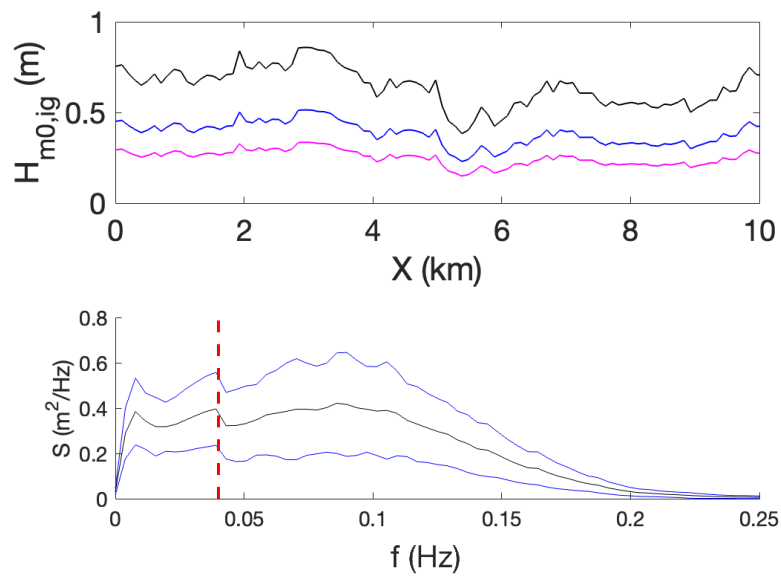


Figure 3.3 Upper panel: Significant FIG (magenta), SWASH-IG (blue) and combined (black) wave height at the reference line at  $Y = 5$  km assuming full reflection. Lower panel: Alongshore averaged surface elevation spectrum of the incident IG waves, i.e. combination of FIG and released IG (black line) plus or minus the standard deviation (blue lines). The delineation between sea-swell and IG waves is given by the red dashed lines in both panels.

## 4 Locally generated bound IG waves

### 4.1 SWAN model set-up

The SWAN model set-up of Deltares (2024) was used to compute the locally generated wind sea in the eastern part of the Wadden Sea. The model extent and input of these models is based on the SWASH models set up by Van Rijnsdorp et al. (2023).

In this study, a uniform wind was applied for two different scenarios<sup>3</sup> and no wave boundary input. An overview of the input conditions for the two model schematizations is shown in Table 4.1. The 2007 storm model input is based on [SWIFT](#) case f150ow07z008, at November 2007, 9:40h, imposing the same constant NAP + 3 m water level as was done for the SWASH computations. For the extreme conditions, Hydra-NL<sup>4</sup> was used to determine the wind conditions for a water level of NAP + 5m.

Table 4.1 Input conditions for the SWAN computations

Domain	Scenario	Wind input	Water level
Lauwersgat	2007 storm	18.44 m/s, 332°N	NAP + 3m
	Extreme conditions (2m SLR)	31.6 m/s, 332°N	NAP + 5 m
Frisian inlet	2007 storm	18.44 m/s, 332°N	NAP + 3m
	Extreme conditions (2m SLR)	34.5 m/s, 332°N	NAP + 5 m

In these computations, the ebb-tidal delta is not taken into account, as we are only considering the locally generated wind waves. The contribution of waves that have been generated outside of the Wadden Sea has been taken into account in Chapter 2.

### 4.2 Wind sea conditions in the Wadden Sea

#### 4.2.1 Lauwersgat

The spatial distribution of the significant wave height computed with SWAN for the Lauwersgat, without IG wave height, is shown in Figure 4.4 for the November 2007 storm scenario (left panel) and for the extreme condition scenario (right panel). No waves were computed from  $Y = 13 - 25$  km, since only the locally (south of the Wadden Sea islands) generated wind waves were considered.

The significant wave height has been shown in Figure 4.2 for two transects: a lateral transect at  $Y = 5$  km and a cross-shore transect at  $X = 3$  km. Both scenarios, the 2007 storm and the extreme scenario, are presented. In the upper panel it can be seen that the waves grow over the cross-shore transect up till a significant wave height of 1 meter for the 2007 scenario and up till almost 2 meters for the extreme scenario. Close to the shore (between  $Y = 2$  and 5 km), the waves break and decrease in size. For the lateral transect the wave height slightly varies, with the highest values near the channel ( $X = 6$  km).

<sup>3</sup> This is different from the SWAN computations of Deltares (2024), where the model schematization included wave boundary conditions, but no wind.

<sup>4</sup> Location WZ\_1\_6-4\_dk\_00193 and WZ\_1\_6-6\_dk\_00050 were used for this purpose.

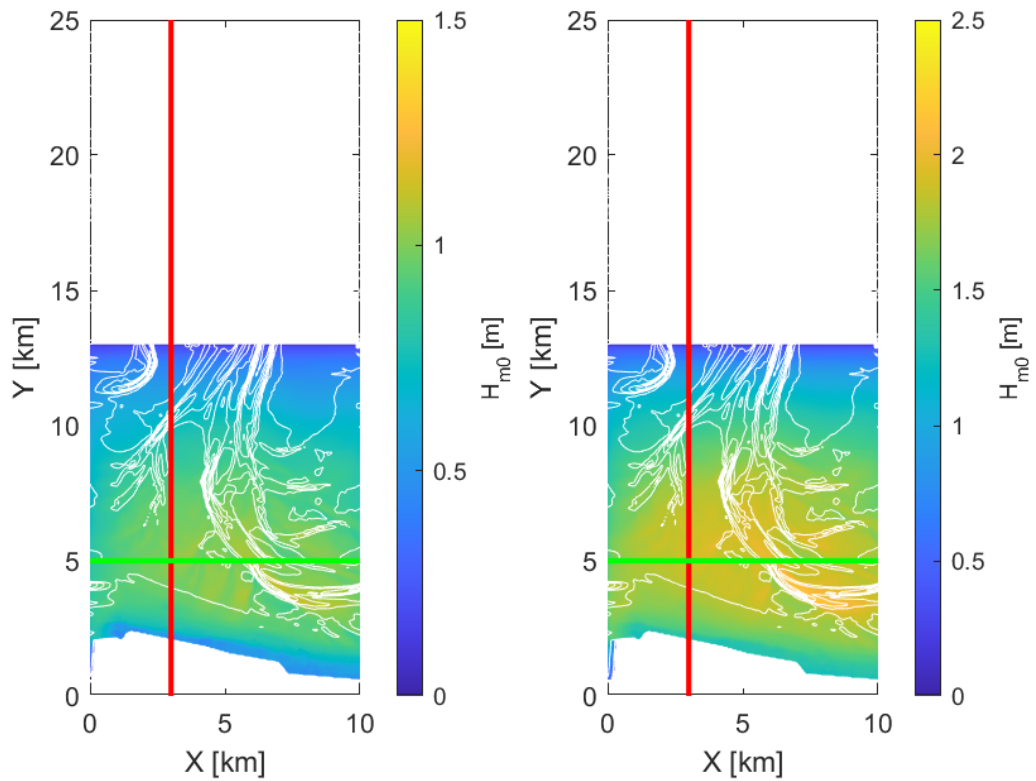


Figure 4.1 Significant wave height during the November 2007 storm condition (left panel) and the extreme condition scenario (right panel) for the Lauwersgat. The colour scales are in m. The lateral transect (reference,  $Y = 5$  km) is given by the green line. The cross shore ( $X = 3$  km) transect is given by the red line.

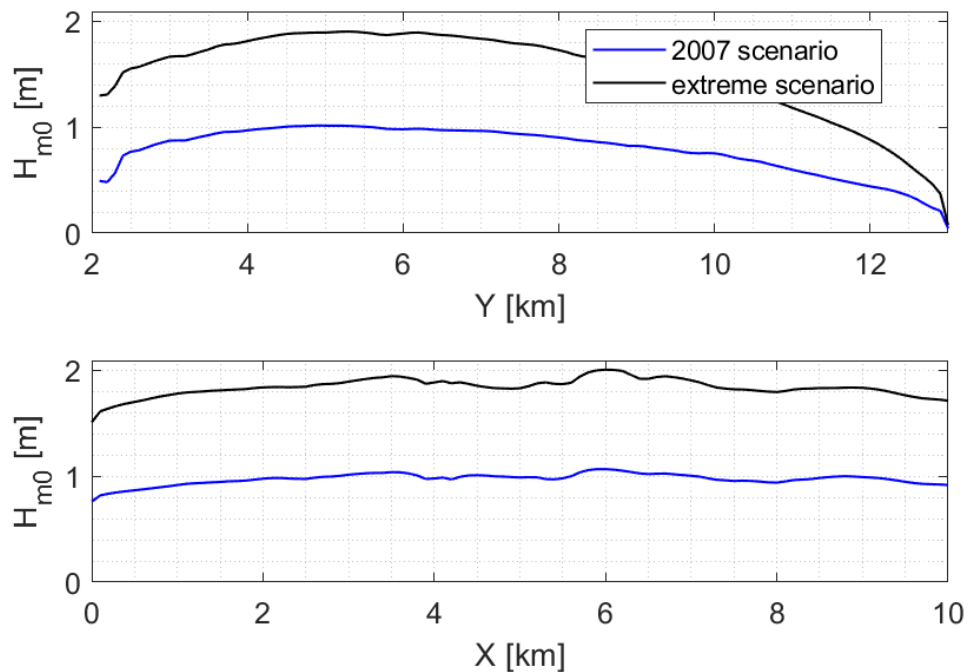


Figure 4.2 Significant wave height along the cross-shore transect  $X = 3$  km (upper panel) and lateral transect  $Y = 5$  km (lower panel) for the 2007 storm condition and the extreme condition scenario in the Lauwersgat .

#### 4.2.2 Frisian inlet

The spatial distribution of the significant wave height computed with SWAN for the Frisian inlet, without IG wave height, is shown in Figure 4.3 for the November 2007 storm scenario (left panel) and for the extreme condition scenario (right panel). No waves were computed from  $Y = 8 - 20$  km, since only the locally (south of the Wadden Sea islands) generated wind waves were considered.

The significant wave height has been shown in Figure 4.4 for two transects: a lateral transect at  $Y = 2$  km and a cross-shore transect at  $X = 12$  km. Both scenarios, the 2007 storm and the extreme scenario, are presented. In the upper panel it can be seen that the waves grow over the cross-shore transect up till a significant wave height of 1 meter for the 2007 scenario and up till almost 2 meters for the extreme scenario. Close to the shore (between  $Y = 0$  and 3 km), the waves break and decrease in size. For the lateral transect the wave height slightly varies, with the highest values near the channel ( $X = 14.5$  km).

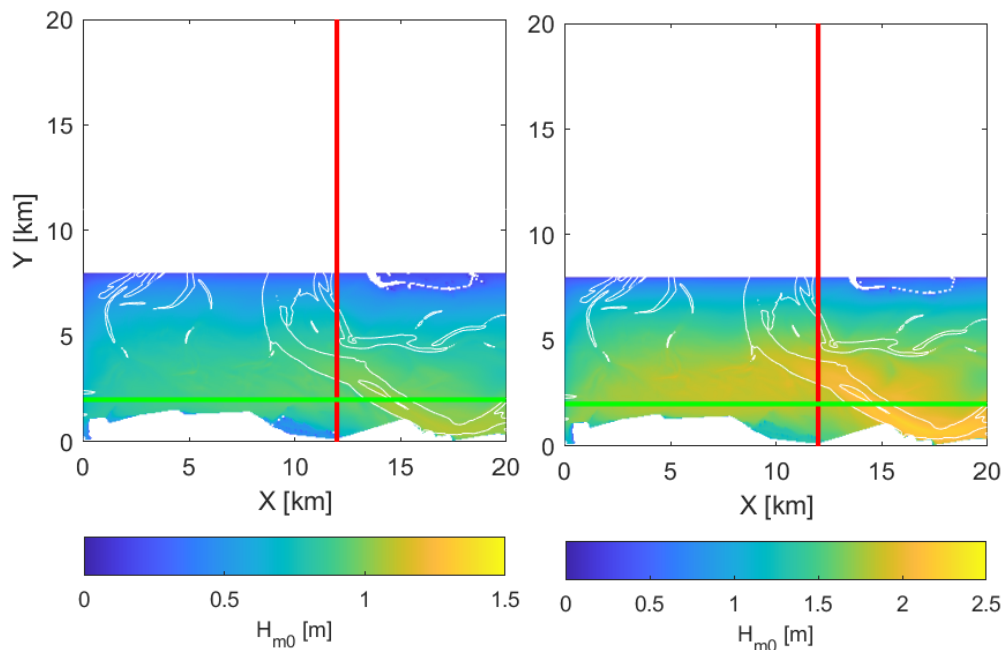


Figure 4.3 Significant wave height during the November 2007 storm condition (left panel) and the extreme condition scenario (right panel) for the Frisian inlet. The colour scales are in m. The lateral transect (reference,  $Y = 2$  km) is given by the green line. The cross shore ( $X = 12$  km) transect is given by the red line.

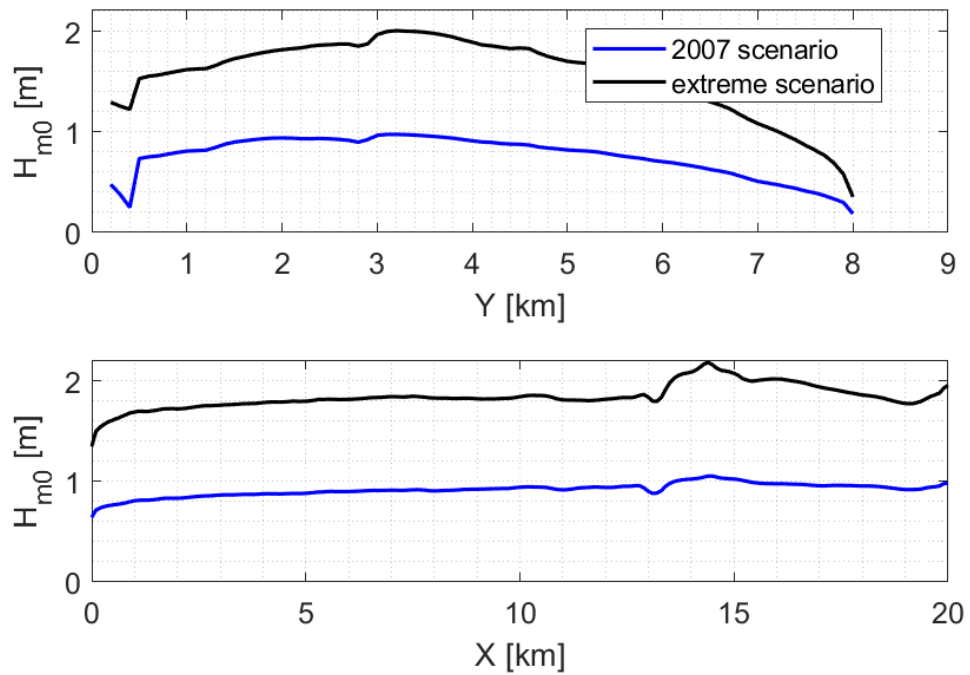


Figure 4.4 Significant wave height along the cross-shore transect  $X = 12$  km (upper panel) and lateral transect  $Y = 2$  km (lower panel) for the 2007 storm condition and the extreme condition scenario in the Frisian inlet.

## 4.3 BIG waves from locally generated wind waves

### 4.3.1 Lauwersgat

The formulae of Hasselmann (1962) have been used to calculate the equilibrium bound IG waves (BIG) along the two transects, using the computed 2D wave energy density spectra from SWAN.

Figure 4.5 shows the results along the two transects (upper panel: cross-shore transect, lower panel: lateral transect) for the 2007 storm scenario and the extreme scenario. For the upper panel it can be seen that the equilibrium bound IG wave height increase along the transect towards the shore ( $Y = 2$  km), with a peak of circa 2 centimetres for the 2007 storm scenario and a peak of approximately 4 centimetres for the extreme scenario. The spike near  $Y = 2$  km may be a spurious result due to limited depth. Along the lateral transect there is some variation due to variations in depth, for example a significant decrease of the equilibrium BIG wave height due to the channel between  $X = 6$  and  $7$  km.

Compared to the component generated by sea-swell (see Chapter 2) and the remotely generated free IG component (see Chapter 3), the locally wind-sea generated bound IG component is a secondary effect and hardly significant.

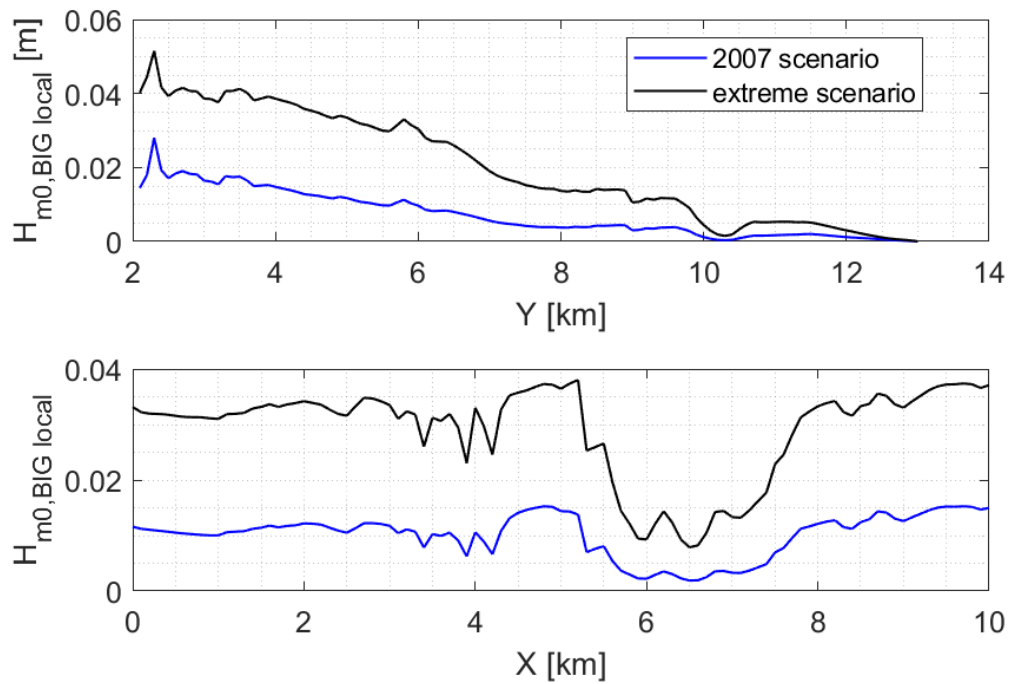


Figure 4.5 Upper panel: IG wave height along the lateral transect in the Lauwersgat for two scenarios. Lower panel: IG wave height along the cross-shore transect in the Lauwersgat for two scenarios.

#### 4.3.2 Frisian inlet

Figure 4.6 shows the results along the two transects (upper panel: cross-shore transect, lower panel: lateral transect) for the 2007 storm scenario and the extreme scenario. For the upper panel it can be seen that the bound IG waves increase along the transect towards the shore ( $Y = 0.2$  km), with maximum values of 2 centimetres for the 2007 storm scenario and 4 centimetres for the extreme scenario. The IG waves are slightly lower at the locations of the channels (between 3 and 4 km and 6 and 7 km). The spike near  $Y = 0.4$  km may be a spurious result due to limited depth. Along the lateral transect there is some variation due to variations in depth, for example a significant decrease of the BIG waves due to the channel between  $X = 13$  and 16 km.

As in the Lauwersgat, the locally wind-sea generated bound IG component is a secondary effect and hardly significant, when compared to the component generated by sea-swell and the remotely generated free IG component.

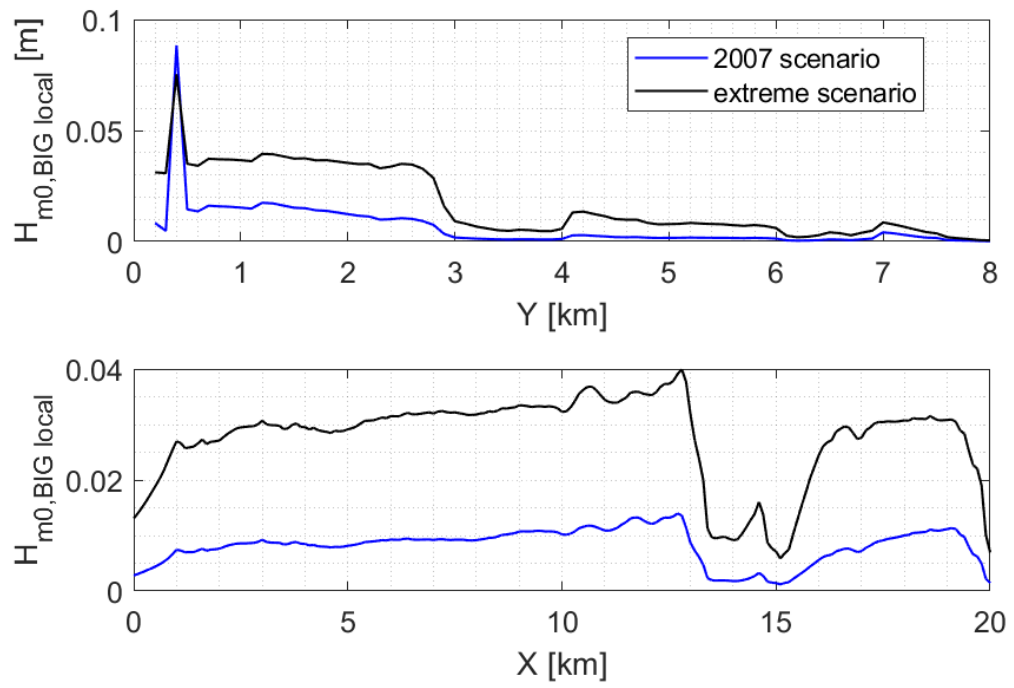


Figure 4.6 Upper panel: IG wave height along the lateral transect in the Frisian inlet for two scenarios. Lower panel: IG wave height along the cross-shore transect in the Frisian inlet for two scenarios.

# 5 Analysis of total IG wave energy

## 5.1 Evolution of remote and locally generated IG waves

In Chapters 2, 3 and 4, three different IG wave contributions have been considered: the released IG waves from the bound sea-swell, the free IG waves, and locally generated bound IG waves. Figure 5.1 shows for every component, the IG wave height in the extreme scenario along the lateral transect ( $Y = 5$  km) in the Lauwersgat. For these wave heights, both the incoming and reflected wave energy has been taken into account for the released IG waves from the bound sea-swell and the free IG waves, as a proxy for the IG wave height at the toe of the dike (the upper panel of Figure 3.3 shows IG wave components at the lateral transect without the reflected component). The total significant IG wave height is shown in Figure 5.1 (black line).

From Figure 5.1 we can conclude that the released IG waves from the bound sea-swell have the largest contribution to the total IG wave height in the Lauwersgat. The total IG wave height has a magnitude between 0.4 and 0.9 meters, depending on bathymetry. Locally generated bound IG waves have the smallest contribution, with magnitudes in the order of centimetres, and can be neglected.

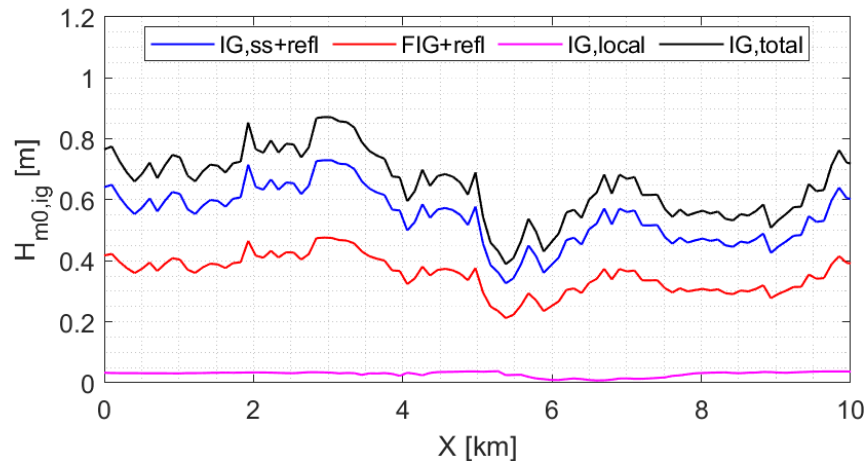


Figure 5.1 Total significant IG wave height (black), combined from three different components for the extreme scenario: released IG waves from the bound sea-swell (ss and reflection, in blue), the free IG waves (and reflection, in red) and locally generated bound IG waves (in magenta) at the lateral transect,  $Y = 5$  km in Lauwersgat.

With the three IG contributions, the energy density spectra of sea-swell and IG waves have been combined, see Figure 5.2. Subsequently, the integral wave parameters have been calculated from the combined energy density spectra.

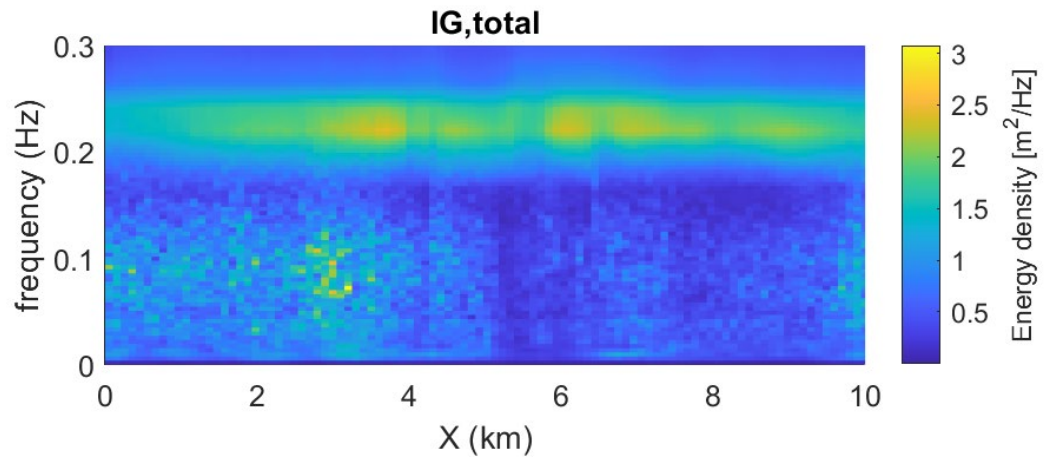


Figure 5.2 Combined energy density spectra (both IG as well as wind sea) at the lateral transect,  $Y = 5$  km in Lauwersgat.

In Chapter 6 the wave run up is computed. As input only the incoming (IG) waves at the toe of the dike are required. In order to obtain the incoming wave components, both wind-wave and IG wave energy need to be shoaled from the  $Y = 5$  km reference line to the toe of the dike. Note that here the IG wave heights excluding the reflected components are used (Figure 3.3). The water depth at the lateral transect is roughly between 5 and 6 metres, with the exception of the water depth in the channel at  $X = 6$  km with 10 to 12 metres. We assumed a water depth near the toe of the dike between 3 and 4 metres, the bed profile being typically at NAP + 1–2 m.

The upper panel of Figure 5.3 compares the total incoming significant wave height with the IG components (black line) near the toe of the dike with the incoming significant wave height without IG components (black dashed line). A difference of approximately 15 centimetres is observed between the two lines. The total IG wave height near the toe of the dike is given in blue, with a total incoming IG wave height of up to 0.7 metres.

In the lower panel, the spectral wave periods  $T_{m-1,0}$ , with and without IG waves, are compared. Differences of 2 to 4 seconds in wave period are observed due to the contribution of the incoming IG waves.

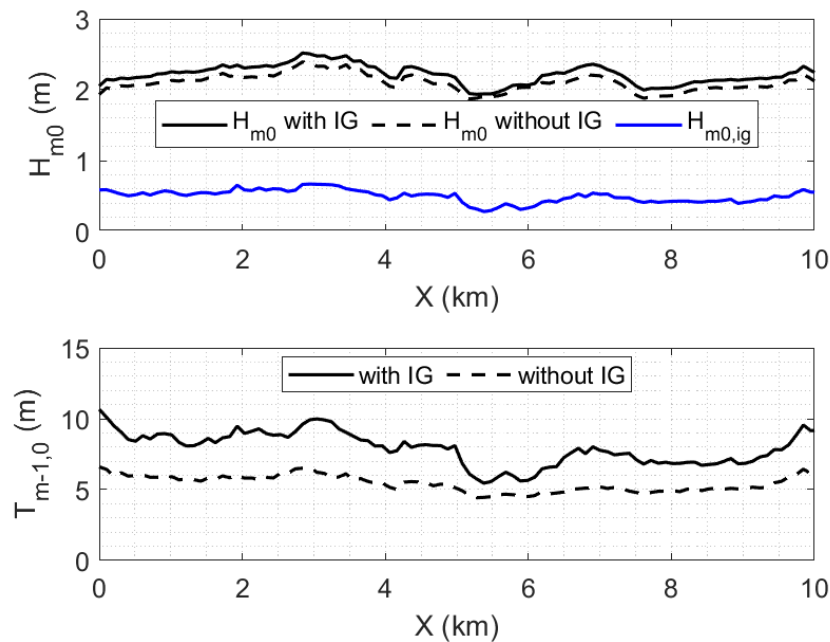


Figure 5.3 Upper panel: Incoming significant wave height with the IG components (black) compared to the significant wave height without the IG components (black dashed line) near the toe of the dike. The total incoming IG wave height is shown in blue, which consists of: released IG waves from the bound sea-swell, the free IG waves and locally generated bound IG waves. The lower panel shows the comparison between the wave period  $T_{m-1,0}$  with (black line) and without (black dashed line) IG waves near the toe of the dike.

Figure 5.1 shows that the total IG wave energy at the reference line is clearly dominated by the remotely generated FIG and the released and bound IG waves generated by the sea and swell at the North Sea. The locally generated IG waves can be neglected, not only at the reference line, but also in the entire inlet. This contribution does not have to be considered when the evolution of the IG waves from offshore to nearshore is analysed. Consequently, Figure 2.10 can be used for further analysis. In Section 3.2, the evolution of the FIG is assumed to be the same as for the released and bound sea swell IG waves. Figure 2.10 shows that the maximum IG wave height is reached at the ebb-tidal delta. The IG wave energy decreases gradually towards the reference line at  $Y = 5$  km. Figure 5.1 shows that the total IG wave height is 0.4 – 0.9 m along this reference line, as a proxy for the IG wave height at the of the dike.

## 5.2 Bandwidth IG waves

In the previous section, the spatial variation of the total IG wave height along the dikes in the Lauwersgat is estimated to be 0.4–0.9 m. The Frisian inlet SWASH computations became unstable for the extreme case. However, for the storm of November 2007 similar IG wave heights have been obtained along the dikes in both inlets. Therefore it is plausible that under extreme conditions, the total IG wave height along the dikes in the Frisian inlet will also be approximately 0.4–0.9 m.

The imposed water level during the November storm is NAP + 3 m and has a return period of less than 10 years. A 2 m higher water level has a return period of 1000 years. The variation of the sea swell component of the IG waves along the reference line in both inlets for the November storm is 0.2–0.3 m, see Figure 2.7 and Figure 2.9. The 1/10 per year offshore FIG wave height is 0.27 m, see Figure 3.1. The total IG wave height along the dikes is estimated to be 0.3–0.5 m, including the effect of shoaling near the dike. Even for this smaller return

period of 10 years, the IG wave height may be significant. In a probabilistic computation of dike erosion not one return period is considered, but the entire exceedance curve of hydraulic loads is relevant.

The estimates above are not only relevant for the Lauwersgat and Frisian inlet. Also for the less sheltered eastern part of the Wadden Sea, the Eems-Dollard excluded, the IG wave height is likely to be of the same order. The Eems-Dollard is more sheltered and IG waves will be hampered to penetrate into this part of the estuary. The IG wave energy will probably be less.

Not only in the north of the Netherlands will bound IG waves be present, but also in the Southern Delta. In front of the Eastern and Western Scheldt, shoals are present, at which waves break and bound IG waves are released. The North Sea waves are smaller and shorter in this region, compared to the area north of the Wadden Sea. Therefore, the bound IG waves in the Southern Delta will be smaller. This also holds for the IG waves being released on the shoal in front of the Eastern Scheldt barrier. Since the water depth between the shoal and the Eastern Scheldt barrier is significantly larger than the shallow Wadden Sea, the decrease of the IG wave height behind the shoal might be less. The IG wave height at the Eastern Scheldt barrier might therefore be of the same order as in front of the Wadden Sea dikes. The FIG wave height is smaller than in the Wadden Sea (TU Delft, 2025). The total IG wave height at the Eastern Scheldt barrier may still be of the same order as in front of the Wadden Sea dikes.

A similar reasoning is valid for the Western Scheldt. However, the directional spreading is much larger than in between the islands of the Wadden Sea. Due to the spreading of the energy the IG wave height may be smaller than in the Wadden Sea.

## 6 Estimate of impact on flood probability

### 6.1 Effect of IG waves on wave run up.

In Section 5.1, the total incoming significant wave height and wave period near the toe of the dike of Lauwersgat was calculated with and without an IG wave contribution (Figure 5.3). With these parameters, wave run-up  $z_{2\%}$  calculations have been done with the formula of Van Gent (2001) for a 1 in 3 slope. The Van Gent (2001) formula only includes the incoming wave energy. In case of the waves including the IG wave contribution, the coefficients  $c_0$  and  $c_1$  for 'Total: long and short waves',  $c_0 = 1.45$  and  $c_1 = 3.8$  have been taken into account. In case of the waves excluding the IG wave contribution<sup>5</sup>, the coefficients  $c_0$  and  $c_1$  for 'Short waves only',  $c_0 = 1.45$  and  $c_1 = 5.0$  have been taken into account.

Figure 6.1 shows the wave run-up for waves with an IG contribution and waves without an IG contribution (upper panel) and the difference between the two (lower panel). Differences in run-up height in the order of 0.8–2 m can be observed.

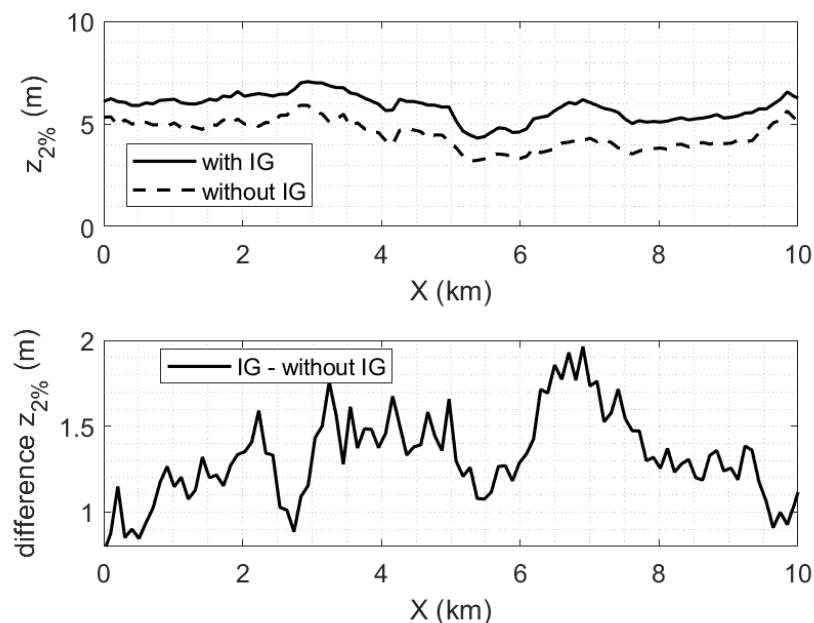


Figure 6.1 Upper panel: wave run-up on the dike of Lauwersgat, calculated with Van Gent (2001) with an incoming  $H_{m0}$  and  $T_{m-1,0}$  including (black line) and excluding (black dashed line) IG waves.

### 6.2 Analysis of the impact of including IG waves

The IG waves can be seen as short-scale variations of the water level. They will affect the location where waves slam on the outer slope of the dike, as well as the wave overtopping discharge and grass erosion of the crest and inner slope. For these two failure mechanisms, here noted as GEBU-Golfklap and GEKB respectively, failure probabilities have been determined for two locations in the Wadden Sea, i.e. Harlingen and Noordpolderzijk. The results of these computations and assumptions made in these computations are described in

---

<sup>5</sup> Meaning that the IG wave energy is not included in the wave energy spectra and resulting integral wave parameters  $H_{m0}$  and  $T_{m-1,0}$ . The IG wave contribution is included implicitly in the wave runup formula by increasing coefficient  $c_1$ .

Appendix A. Here we consider the results at Noordpolderzijl, located in the eastern part in the Wadden Sea.

In Section 5.2, the total (incident and reflected) IG wave height was estimated between 0.5 and 0.9 m. From Table A-2 and A-4 we may conclude that inclusion of IG waves will lead to an increase of the failure probability by a factor 1.5–2 and 2–5 for GEKB and GEBU-Golfklap respectively. This is considered as a lower limit, as will be discussed in the next paragraph.

## 6.3 Discussion

In this study various assumptions have been made related to the combined wave modelling with SWASH and SWAN, see Section 1.3. The consequence of other assumptions are briefly discussed below.

The offshore FIG wave height is determined from a statistical analysis by TU Delft (2025) and transformed onshore by assuming the same spatial evolution as the sea-swell induced bound IG waves that are partly released on the ebb-tidal deltas. Although this may be a strong assumption, the resulting range of FIG seems reasonable and is useful for this study.

The determined range of IG waves is based on available results of SWASH and SWAN computations in two inlets during a storm and an extreme scenario. If more storms and more extreme scenarios would have been considered, probably a wider range of IG wave heights would have been obtained. However, the pattern of increasing IG waves on the ebb-tidal delta and gradual decrease of the IG wave height evolution towards the considered reference line and slight increase due to shoaling is not storm-specific. The range of IG wave height will strongly be determined by the range of the offshore sea swell wave conditions, which lead to generation of BIG - and FIG on other coasts.

The offshore wave conditions that have been imposed at the offshore SWASH and SWAN model boundaries are wave spectra measured at the SON buoy during the November 2007 storm. The significant wave height and peak wave period are 8 m and 16 s respectively. The same conditions have been used as boundary condition for the extreme scenario. In WL (2004), extreme value distributions for the significant wave height and peak period have been determined for SON. The values mentioned above have a return period of 80 years, as can be inferred from Tables B-2 and B-5 in WL (2004). The same distributions show that the values with a return period of 10,000 years equal 11 m and 20 s respectively. These wave conditions will lead to higher offshore IG wave heights. The FIG component will be unaltered, so the total IG wave height at the reference line will also increase. This also holds for the failure probability. The increase in failure probability presented in Paragraph 6.2 can be considered as a lower boundary of what can be expected for the more extreme conditions.

## 7 Conclusions

Results from available SWASH and SWAN hindcasts of the November 2007 storm and an extreme scenario based on that same storm have been analysed to estimate the range of IG wave height in front of the dikes in the Wadden Sea. Based on the analysis we conclude that for the extreme scenario (approximately a 1:10,000 year event):

- The total (incident and reflected) IG wave height in front of the dikes is 0.4–0.9 m. The released IG waves that were originally bound to the sea-swell at the North Sea has the largest contribution, the FIG wave height is slightly smaller, but in the same order of magnitude. The IG waves bound to the locally generated wind sea is only a few centimetres and can be neglected.
- The sea-swell from the North Sea contains bound IG waves that are released on the slope of the ebb-tidal delta, reach their maximum wave energy on the ebb-tidal delta, which gradually decreases over the shallow region towards the dikes and shoal slightly on the shallow foreshore in front of the dike.
- The effect on the wave runup height  $z_{2\%}$  is 0.8–2.0 m.
- The failure probability for the mechanisms GEKB and GEBU-Golfklap increases with a factor 1.5–2 and 2–5 respectively, which can be considered as a lower boundary of what can be expected for the more extreme conditions. If offshore wave boundary conditions, including IG waves, would have been considered that are consistent with the extreme water level considered, these factors would have been larger.

For the less sheltered eastern part of the Wadden Sea, the Eems-Dollard excluded, the IG wave heights are likely to be of the same order. The same holds for the IG wave heights in front of the Eastern Scheldt barrier. In the Western Scheldt they are probably smaller.

It should be noted that the conclusions are based on a very limited amount of computations: for one moment during one storm, and a single extreme scenario in two inlets in the Wadden Sea. Also, various assumptions have been made, with respect to the evolution in FIG from offshore to nearshore, regarding the determination of the failure probabilities, in combining the various IG contributions, etc.

The resulting effect on the failure probabilities for GEBU-Golfklap and GEKB is significant. It is recommended to implement IG waves in BOI, so that a more realistic estimate of the run-up and overtopping of dikes is obtained.

## 8 References

- Akrish, G., A. Reniers, D. Rijnsdorp, M. Zijlema, J. Rutten and M. Tissier (2025). The importance of free infragravity waves in the North Sea: Insights from field observations and unstructured SWAN modelling, *Ocean Modelling*, Vol. 198, 102619, ISSN 1463-5003, <https://doi.org/10.1016/j.ocemod.2025.102619>.
- De Ridder, M.P., D. C.P. van Kester, R. van Bentem, D. Y.Y. Teng, M.R.A. van Gent (2024). Wave overtopping discharges at rubble mound structures in shallow water. *Coastal Engineering*, Volume 194 (<https://doi.org/10.1016/j.coastaleng.2024.104626>)
- Deltares (2021). Probabilistisch beoordelen en ontwerpen grasbekleding. Samenvoegen GEBU en GEKB. Deltares rapport 11206202-002, juli 2021 (A.J. Smale en W.J Klerk).
- Deltares (2024). Study to improve low frequency wave penetration in SWAN: Validation of the DCTA method. Deltares report 11208057-017, April 2024 (M. Doeleman and J. Groeneweg).
- Hasselmann, K. (1962). On the non-linear energy transfer in a gravity-wave spectrum: I. General theory, *J. Fluid Mech*, Vol. 12, 481–500.
- Herbers, T.H.C. and Elgar, Steve and Guza, R.T. (1994). Infragravity-frequency (0.005--0.05 Hz) motions on the shelf. Part I: Forced waves, *J. of Phys. Oceanography*, Vol. 24 (5), 917-927.
- Lashley, C.H., J.D. Bricker, J. van der Meer, C. Altomare and T. Suzuki (2020). Relative magnitude of Infragravity waves at coastal dikes with shallow foreshores: A prediction tool. *Journal of Waterway, Port, Coastal, and Ocean Engineering*. Vol. 146 (5). [https://doi.org/10.1061/\(ASCE\)WW.1943-5460.000057](https://doi.org/10.1061/(ASCE)WW.1943-5460.000057).
- Rijnsdorp, D., A. Reniers and M. Zijlema (2023). Collection of reports for Rijkswaterstaat: swell penetration into tidal inlets and the influence of sea level rise.
- Rijnsdorp, Smit and Guza, 2024. A nonlinear, non-dispersive energy balance for surfzone waves: infragravity wave dynamics on a sloping beach. *J. Fluid Mech.*, Vol. 944 (A45), doi:10.1017/jfm.2022.512
- TU Delft (2025). Free infragravity waves along the Dutch coast, SWAN-based estimates for extreme conditions. Work in progress by M. Tissier., M. Zijlema and A. Reniers.
- Van Gent, M.R.A., 2001. Wave runup on dikes with shallow foreshores. *J. Waterway, Port, Coastal, Ocean Eng.*, 127(5), 254 – 262. doi: [https://doi.org/10.1061/\(ASCE\)0733-950X\(2001\)127:5\(254\)](https://doi.org/10.1061/(ASCE)0733-950X(2001)127:5(254))
- WL (2004). Golfstatistiek op relatief diep water 1979 – 2002. WL | Delft Hydraulics rapport Q2770, december 2004 (A.H. Weerts en F.L.M. Diermanse).

# A Effect of IG waves on dike erosion

The so-called GEBU-GEKB<sup>6</sup> tool (Deltares, 2021) has been applied to determine the failure probability due to erosion of revetments on the outer and inner dike slopes. The tool needs the temporal variation of the water level as input. In coastal regions the water level is determined by storm surge and tide, often schematized as the blue line in Figure A.1. The IG waves form short-scale variations of that water level. The effect of IG waves is incorporated by increasing the water level by a part of the IG wave amplitude: for GEKB 50%, for GEBU-Golfklap 90%. The increase of the water level is incorporated as decrease of the crest height of the dike. This approach was based on De Ridder et al. (2024), who described various formulations for wave overtopping that include the effect of IG waves. The formulation getting closest to the measured overtopping discharges is one in which the free board is decreased by a part of the IG wave height. The sensitivity for the selected values 50% and 90% have not been investigated, since the impact on the effect of IG waves on the failure probability may be small.

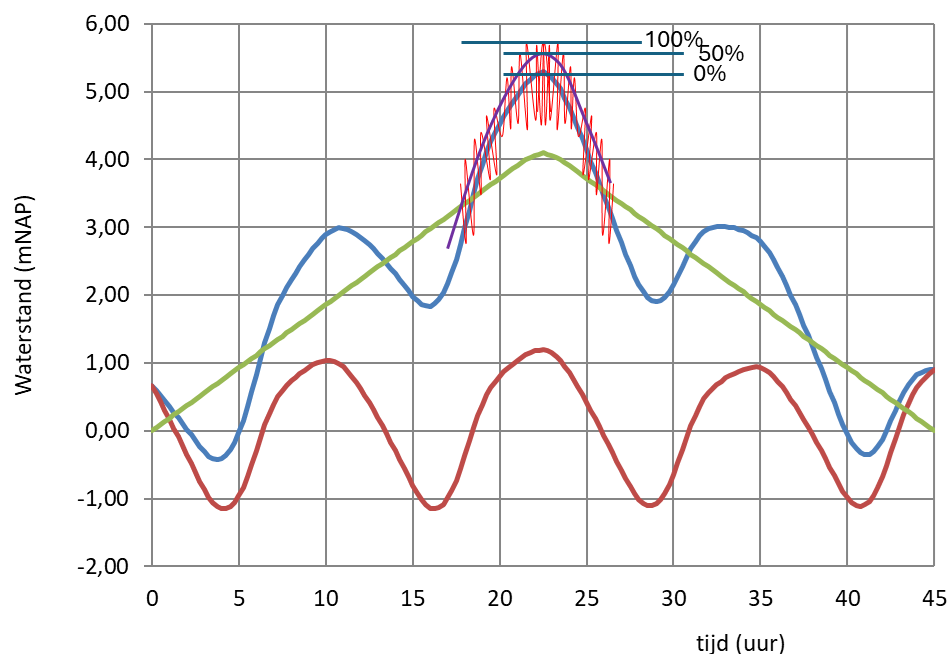


Figure A.1 Schematization of the storm surge (green), tide (red) and resulting water level (blue). The IG waves cause a short-scale variation of the water level.

For two locations in the Wadden Sea the failure probabilities for the failure mechanisms GEKB and GEBU-Golfklap have been determined for a range of IG wave heights and resulting water level increase. For GEKB and GEBU-Golfklap an IG wave height of  $x$  m leads to an imposed increase of the water level of  $0.25x$  m and  $0.45x$  m respectively. The two locations are Harlingen in the western part of the Wadden Sea and Noorpolderzijk in the eastern part. The computed failure probabilities for both failure mechanisms and two locations have been given in Table A-1 – A-4.

<sup>6</sup> GEKB is an abbreviation of “Graserosie Kruin en Binnentalud”, i.e. grass erosion of the crest and inner slope; <sup>6</sup> GEBU is an abbreviation of “Graserosie Kruin Buitentalud”, i.e. grass erosion of the outer slope. The failure mechanism considered in this study is GEBU-Golfklap, i.e. wave impact.

Table A-1 Failure probabilities for GEKB at Harlingen for a range of IG wave heights, implemented as 25% increase of the water level in the GEBU-GEKB tool. The final column denotes the increase in failure probability due to the presence of IG waves.

IG wave height [m]	Water level increase [m]	Pf [1/year]	Factor Pf
0	0	1.2E-08	1.0
0.4	+0.1	1.6E-08	1.4
0.8	+0.2	2.2E-08	1.8
1.2	+0.3	2.9E-08	2.5
1.6	+0.4	4.0E-08	3.4
2	+0.5	5.4E-08	4.6

Table A-2 Failure probabilities for GEKB at Noordpolderzijl for a range of IG wave heights, implemented as 25% increase of the water level in the GEBU-GEKB tool. The final column denotes the increase in failure probability due to the presence of IG waves.

IG wave height [m]	Water level increase [m]	Pf [1/year]	Factor Pf
0	0	2.4E-07	1.0
0.4	+0.1	3.1E-07	1.3
0.8	+0.2	4.0E-07	1.7
1.2	+0.3	5.2E-07	2.2
1.6	+0.4	6.8E-07	2.8
2 m	+0.5	8.8E-07	3.7

Table A-3 Failure probabilities for GEBU-Golfklap at Harlingen for a range of IG wave heights, implemented as 45% increase of the water level in the GEBU-GEKB tool. The final column denotes the increase in failure probability due to the presence of IG waves.

IG wave height [m]	Water level increase [m]	Pf [1/year]	Factor Pf
0	0	3.0E-06	1.0
0.2	0.09	4.6E-06	1.6
0.5	0.225	8.4E-06	2.8
1	0.45	2.5E-05	8.3
1.5	0.675	7.0E-05	23.5

Table A-4 Failure probabilities for GEBU-Golfklap at Noordpolderzijl for a range of IG wave heights, implemented as 45% increase of the water level in the GEBU-GEKB tool. The final column denotes the increase in failure probability due to the presence of IG waves.

IG wave height [m]	Water level increase [m]	Pf [1/year]	Factor Pf
0	0	6.1E-06	1.0
0.2	0.09	8.4E-06	1.4
0.5	0.225	8.2E-06	1.4
1	0.45	2.8E-05	4.6
1.5	0.675	5.5E-05	9.0

Deltares is an independent institute for applied research in the field of water and subsurface. Throughout the world, we work on smart solutions for people, environment and society.

**Deltares**

[www.deltares.nl](http://www.deltares.nl)